# Interannual/decadal variability of South tropical Indian Ocean: natural vs. forced Response

Abhisek Chatterjee,
Anjana S, Prerna Singh and Sajidh C K

Indian National Centre for Ocean Information Services, Hyderabad

Climate Change Workshop, IITM, Pune on 28th November, 2019

# Indian Ocean is warming much rapidly compare to the other tropical basins

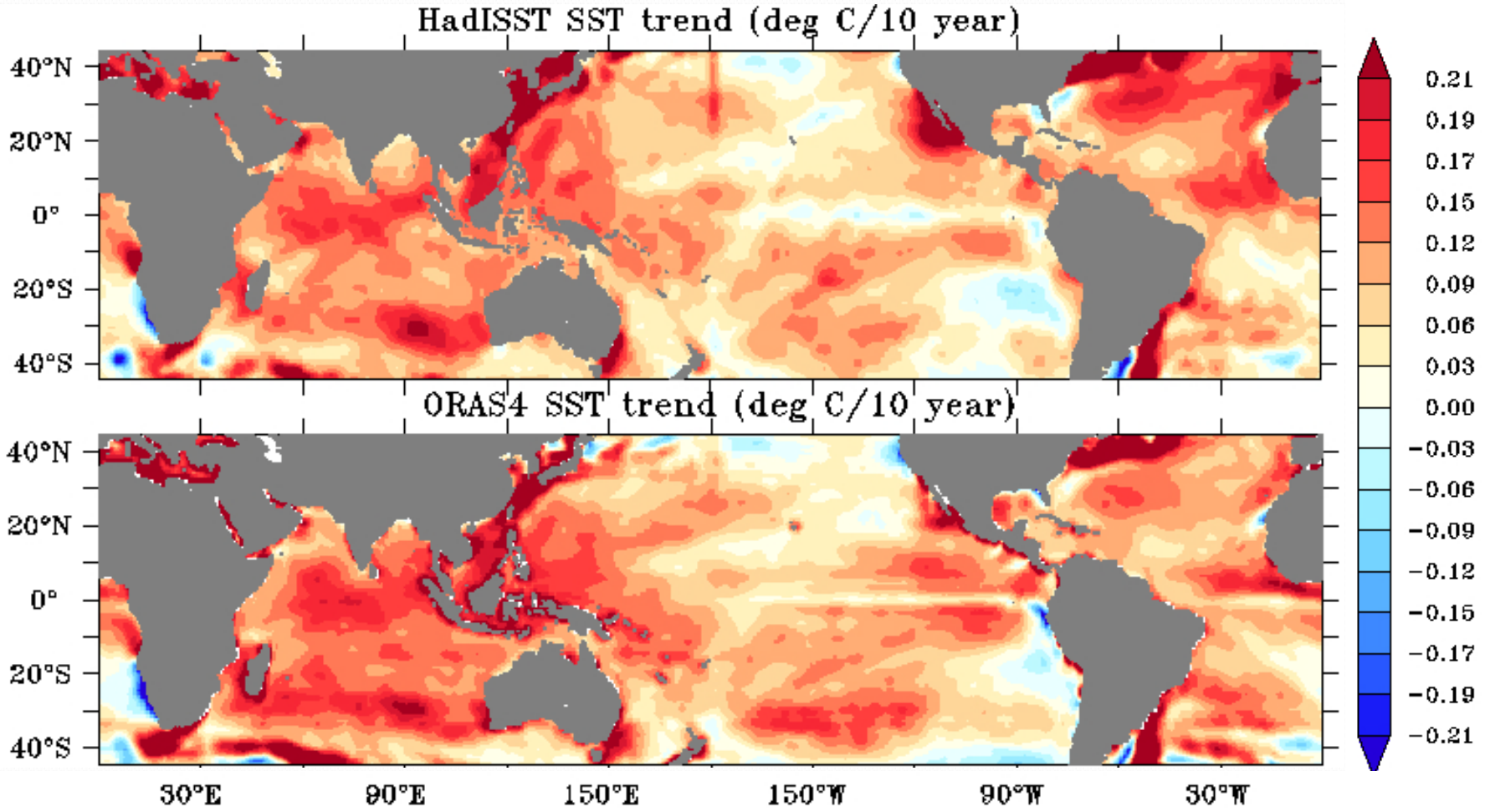

# Indian Ocean is warming much rapidly compare to the other tropical basins

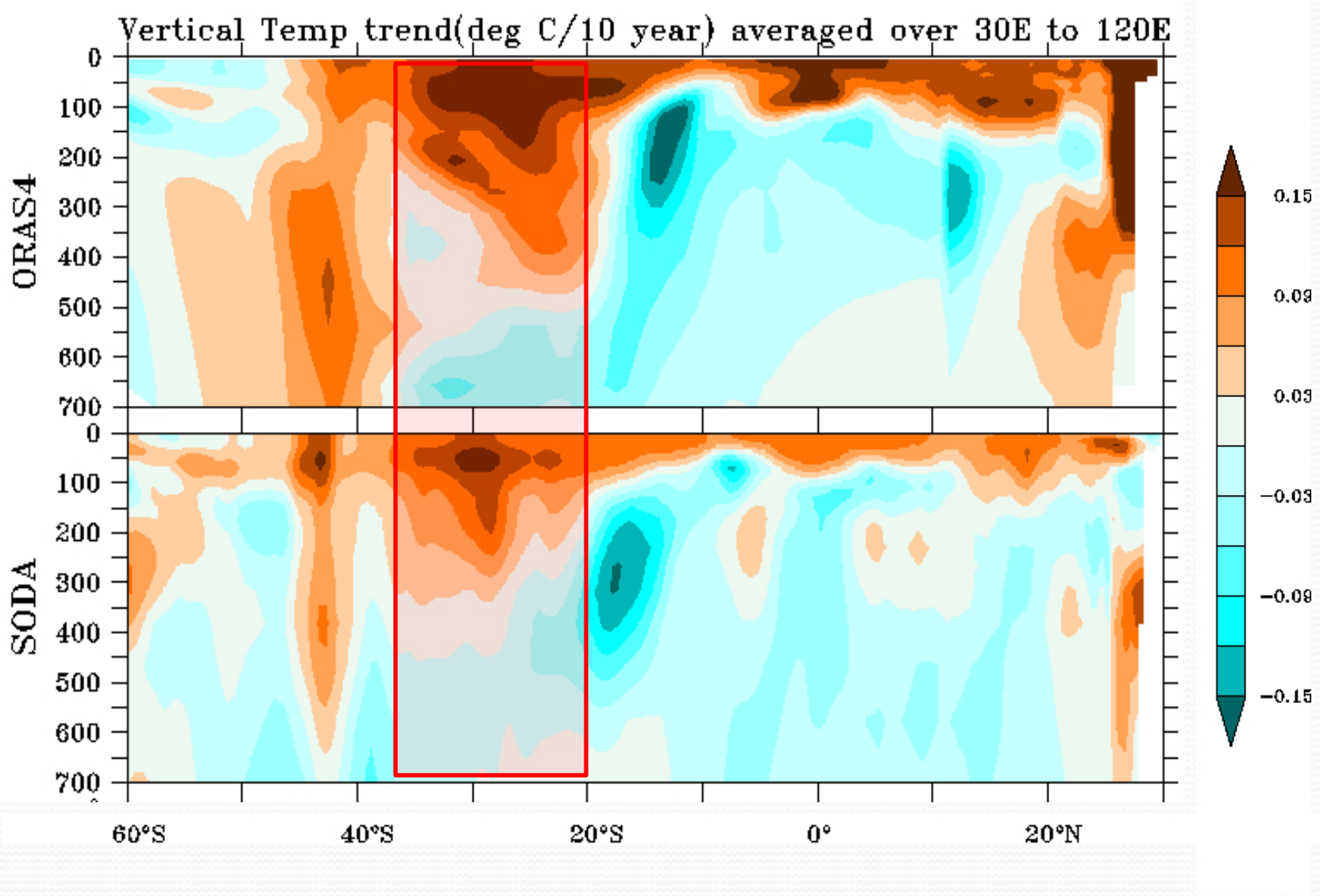

# Heat content of the top 700 m for the Indian Ocean

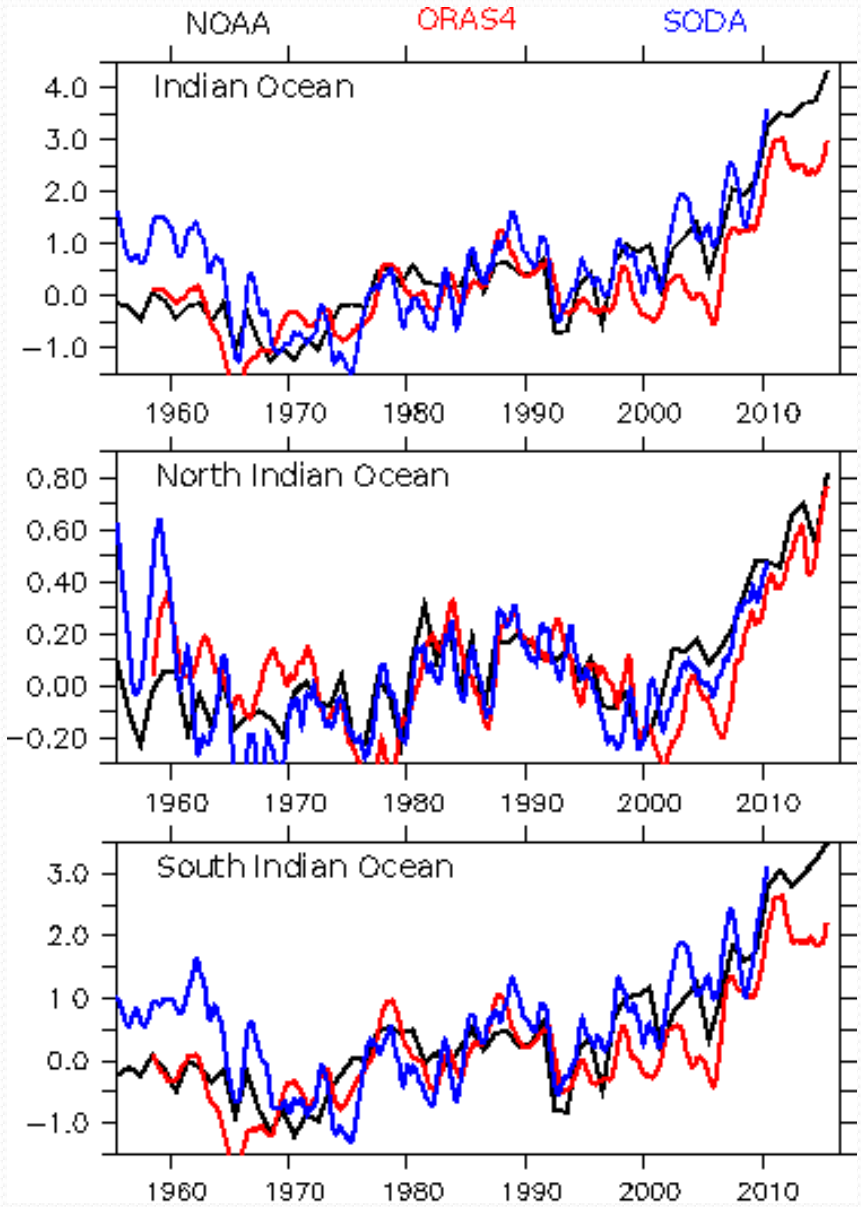


Heat content of top 700 m water column (OHC700; $10^{22}$ J) for the Indian Ocean (20-120E/75S-30N), North Indian Ocean (20-120E/0-30N, except SCS) and South Indian Ocean (20-120E/75S-0N).

Note that, for the north Indian Ocean, OHC700 started rising from late 1970's till 1990 and then indicates a decreasing trend till 2000. However, post 2000, it has increased rapidly.

Interestingly, both the reanalysis products capture the interannual/decadal variability quite well.

# Prominent modes of Indian Ocean interannual variability

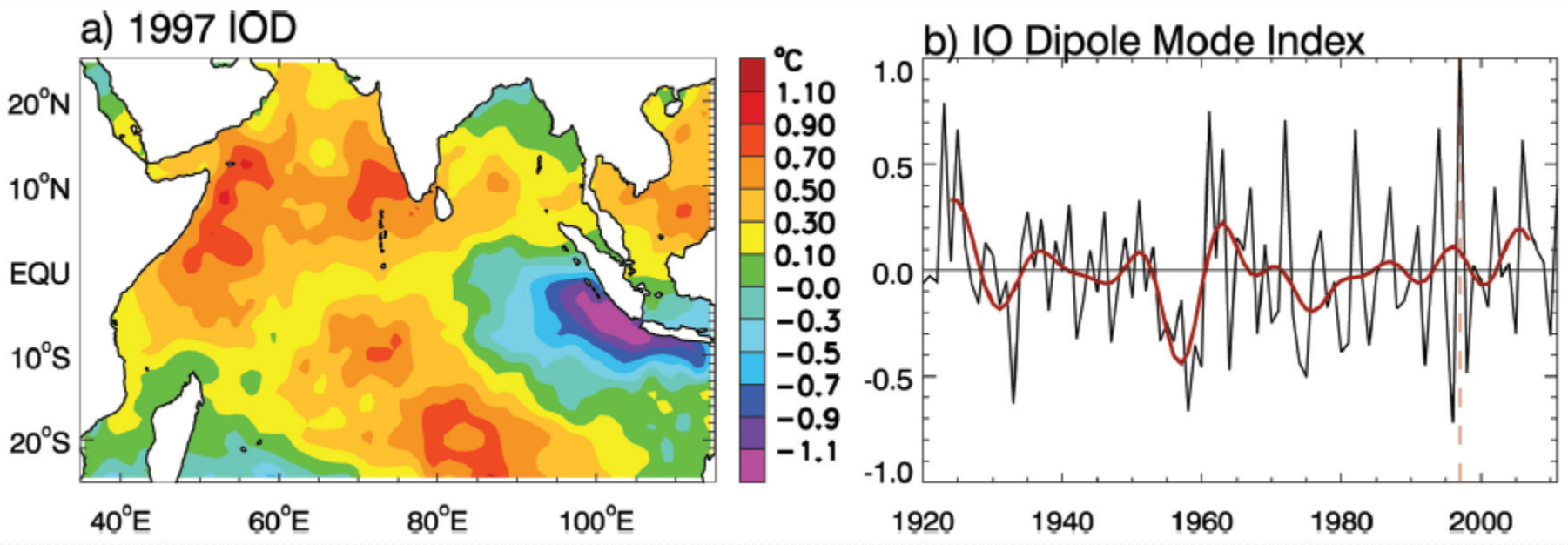


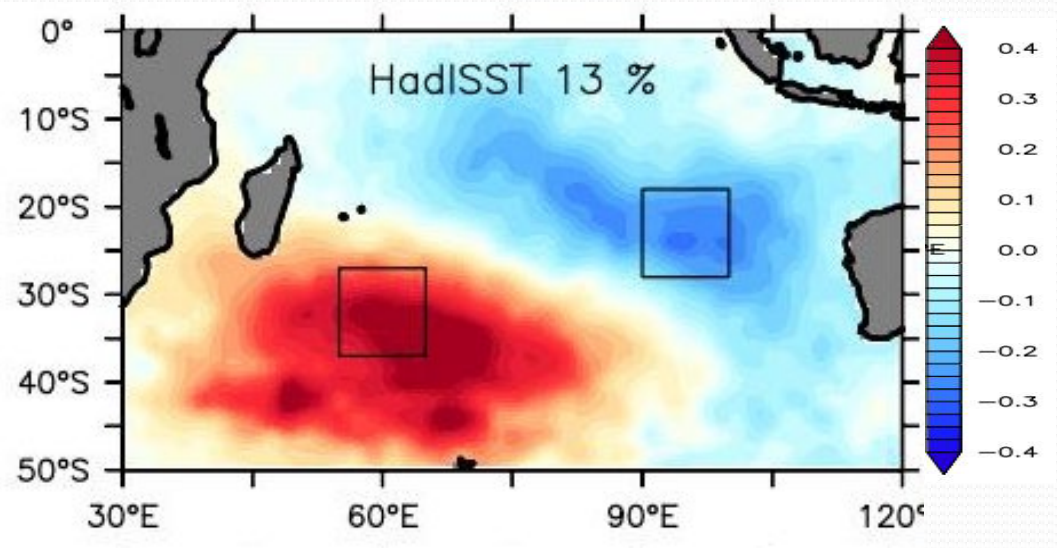

# EOF's of Indo-Pacific sea level anomaly

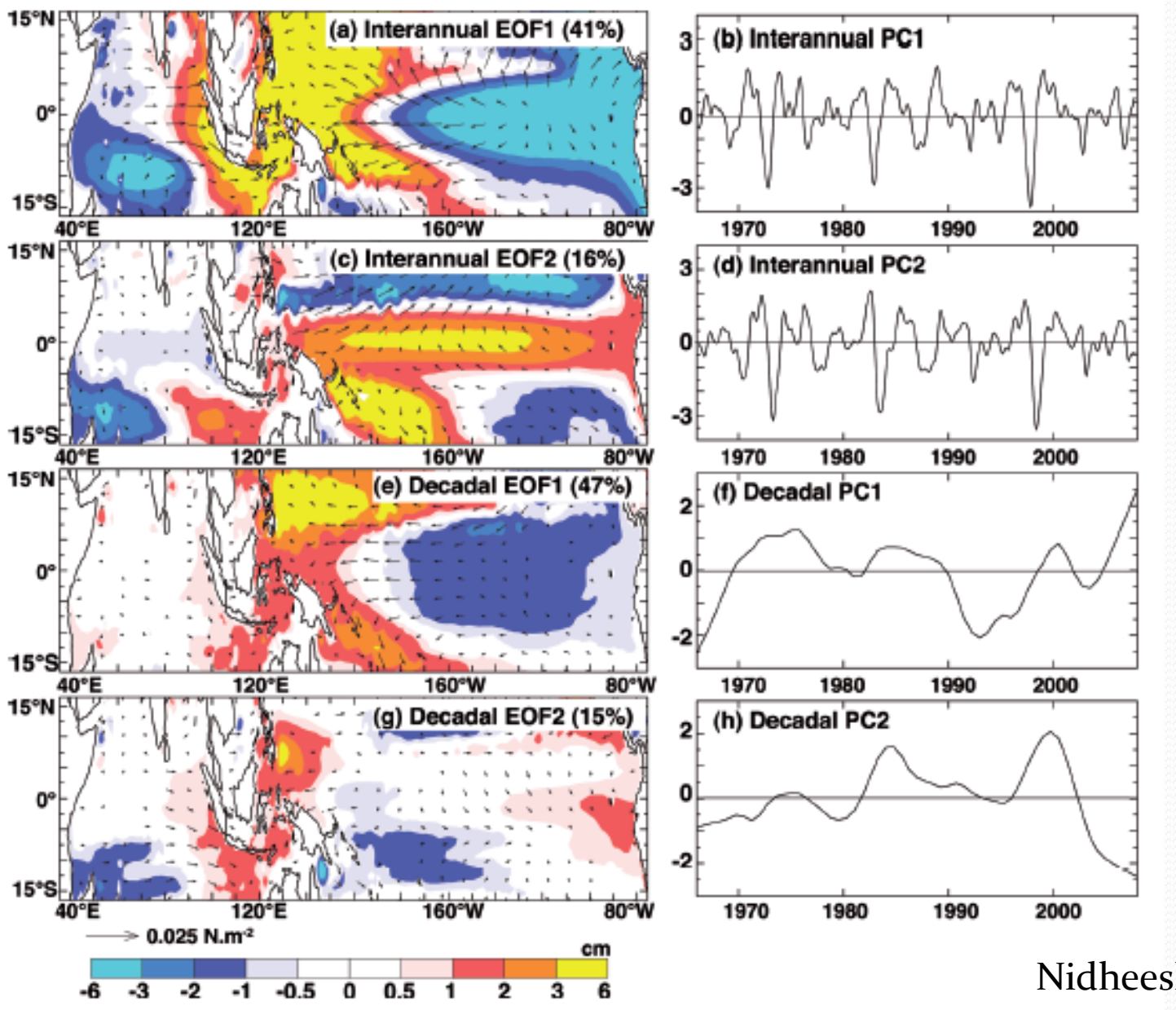


Nidheesh et al., 2013

# EOF's of Indo-Pacific sea surface temperature anomaly

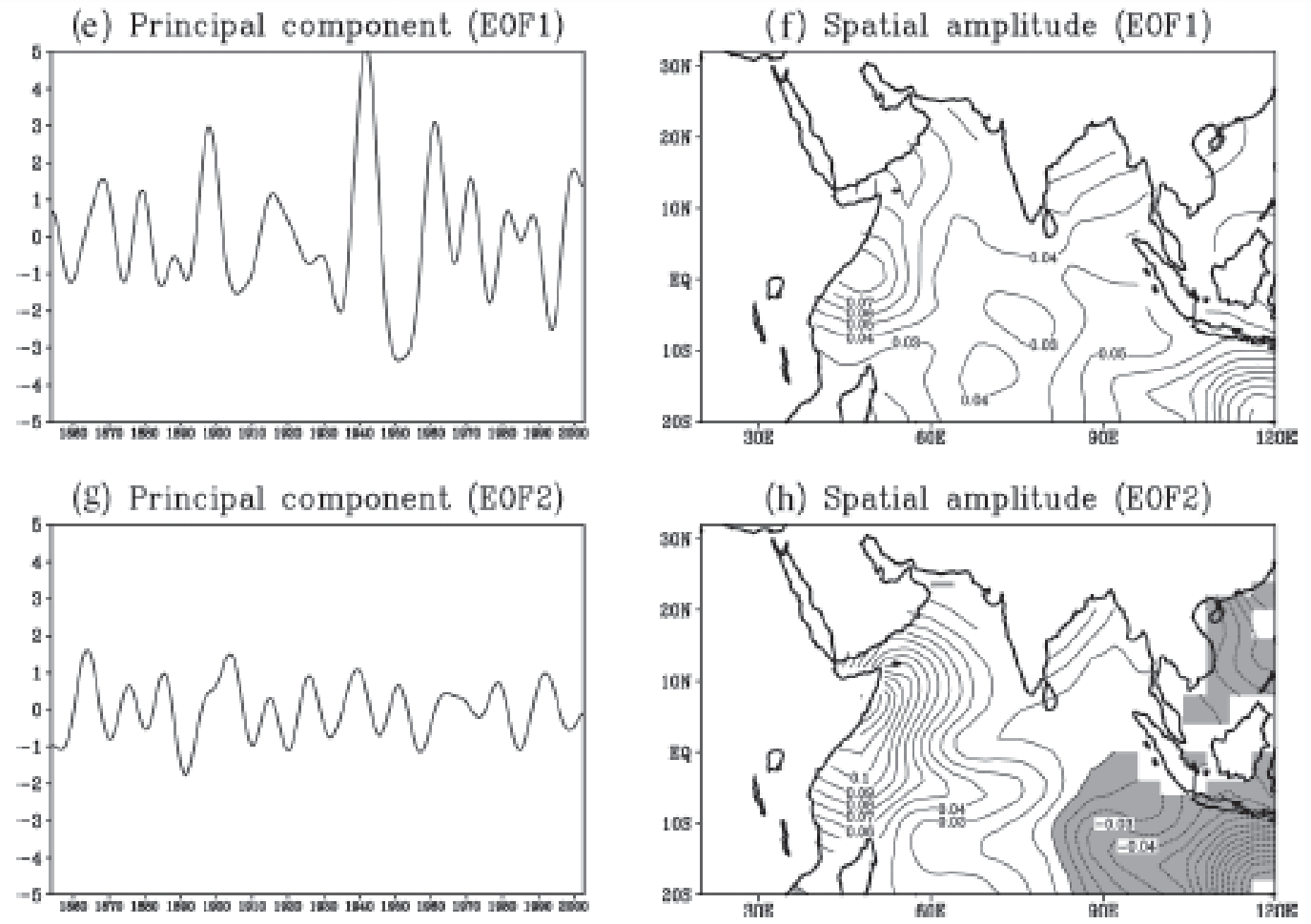


Han et al., 2014

# While natural mode of decadal variability studied extensively for Pacific/Atlantic Ocean, Decadal variability of the IO is much less explored.

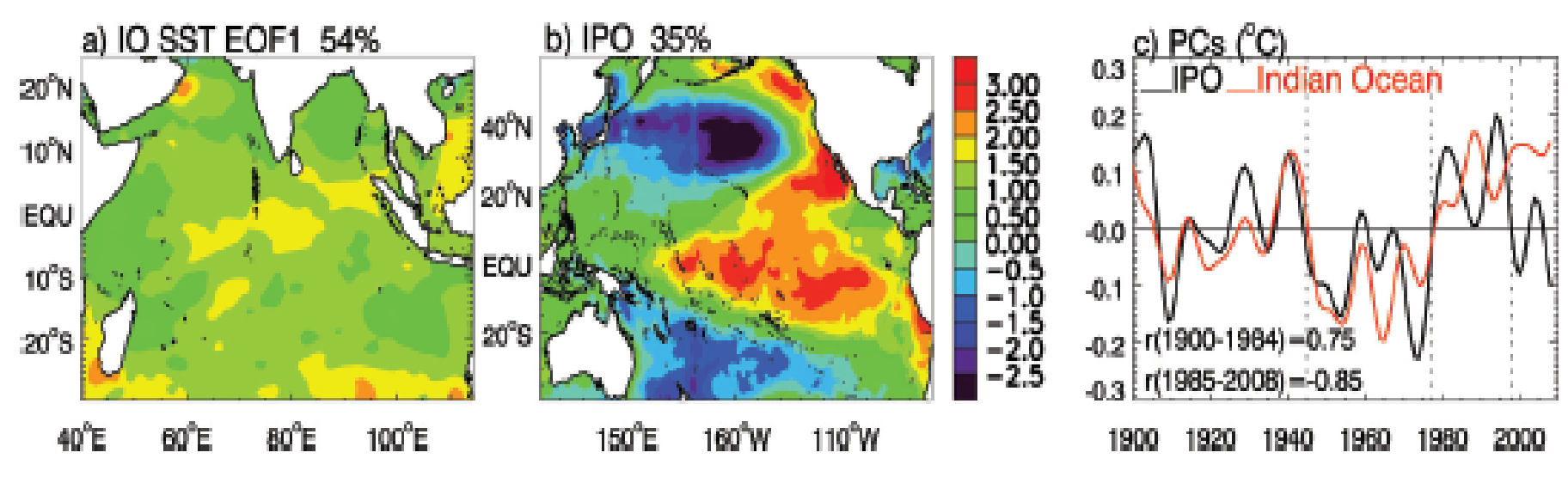


Indo-Pacific atmospheric bridge explains the co-occurrence of two leading mode of Pacific and IO up to until 1985. The correlation reverses afterwards.

Han et al., 2014

# While natural mode of decadal variability studied extensively for Pacific/Atlantic Ocean, Decadal variability of the IO is much less explored.

Leading EOFs of sea level anomaly from the ensemble mean of CMIP models.

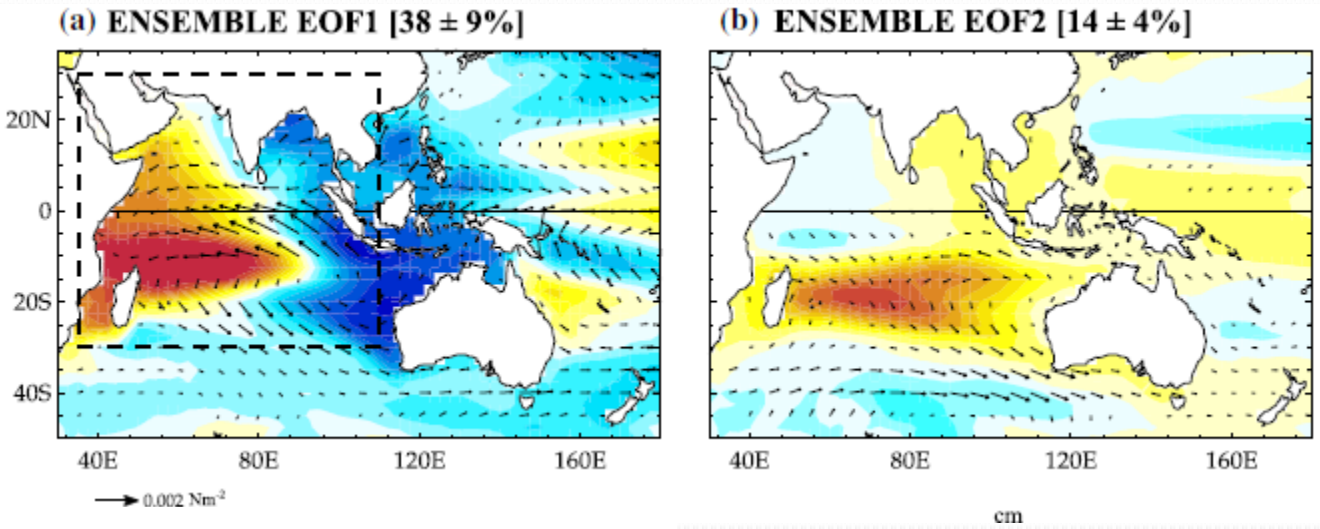


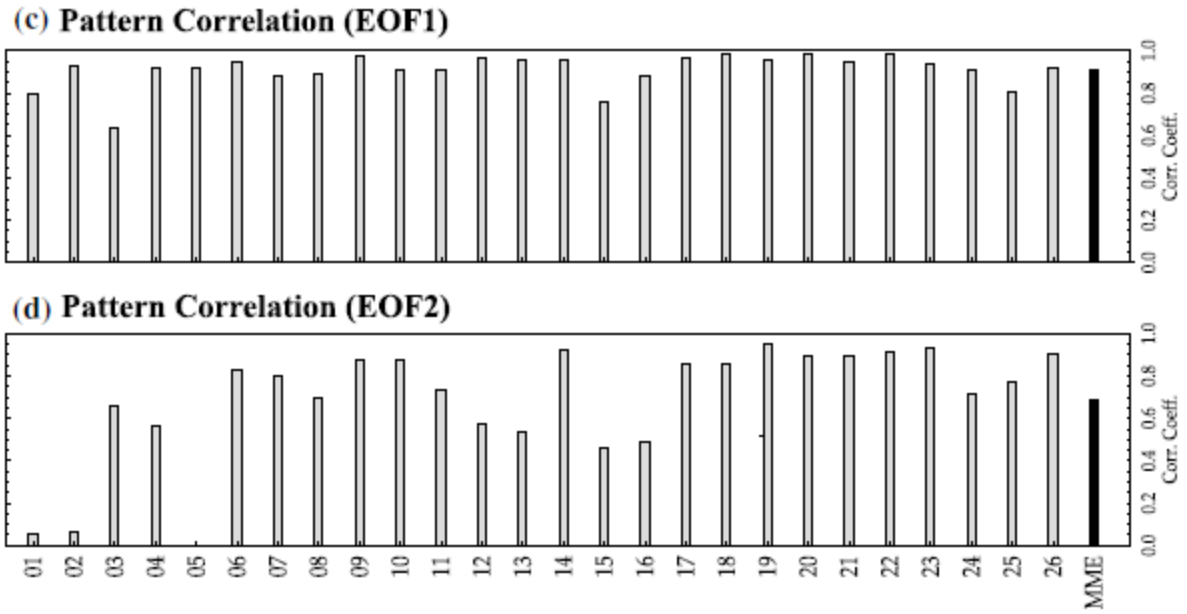


While the first mode is quite robust across the model, discrepancies are large for the second mode.

Nidheesh et al., 2019

# While natural mode of decadal variability studied extensively for Pacific/Atlantic Ocean, Decadal variability of the IO is much less explored.

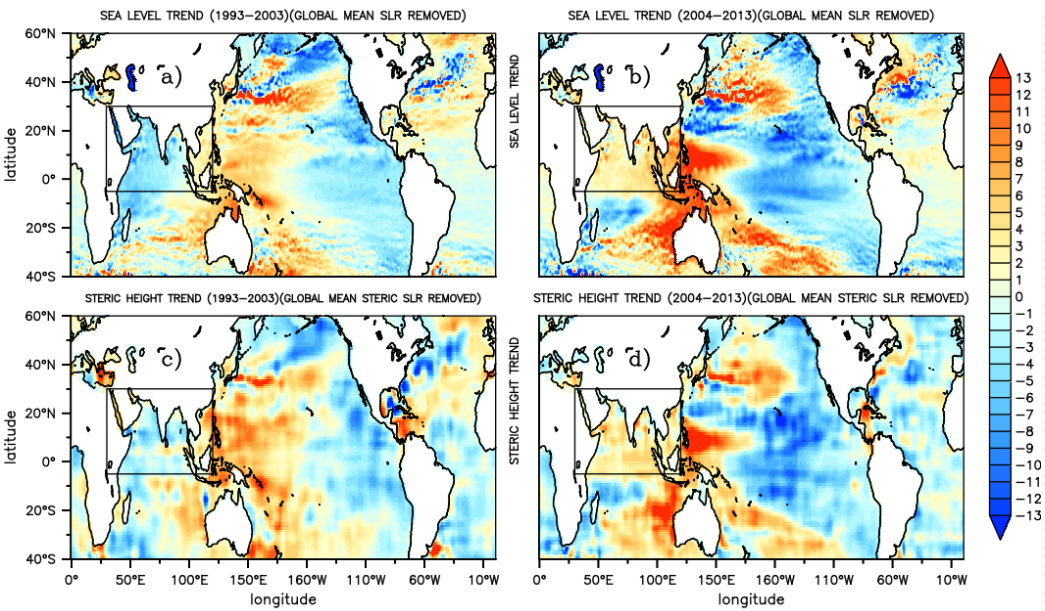


*Satellite observed spatial pattern of sea level trend (with global mean SLR removed) from AVISO data for the period of a 1993-2003 (Period-I), and b 2004-2013 (Period-II); c and d are the same as a and b, respectively, except for 0-700 m steric (thermal + halo) sea level trends from EN4 data. The rectangular box in each panel shows the region of decadal reversal of sea level, which is north of 5 ° S.*

This reversal of sea level trend is explained by the change in the winsdtress curl over the north IO that resulted in decadal change in the transport through the shallow cross equatorial cell.

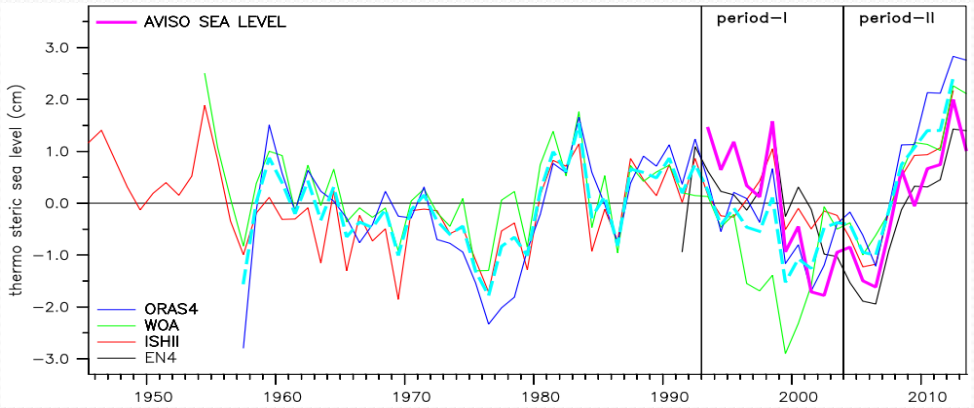


Srinivasu et al., 2016

# While natural mode of decadal variability studied extensively for Pacific/Atlantic Ocean, Decadal variability of the IO is much less explored.

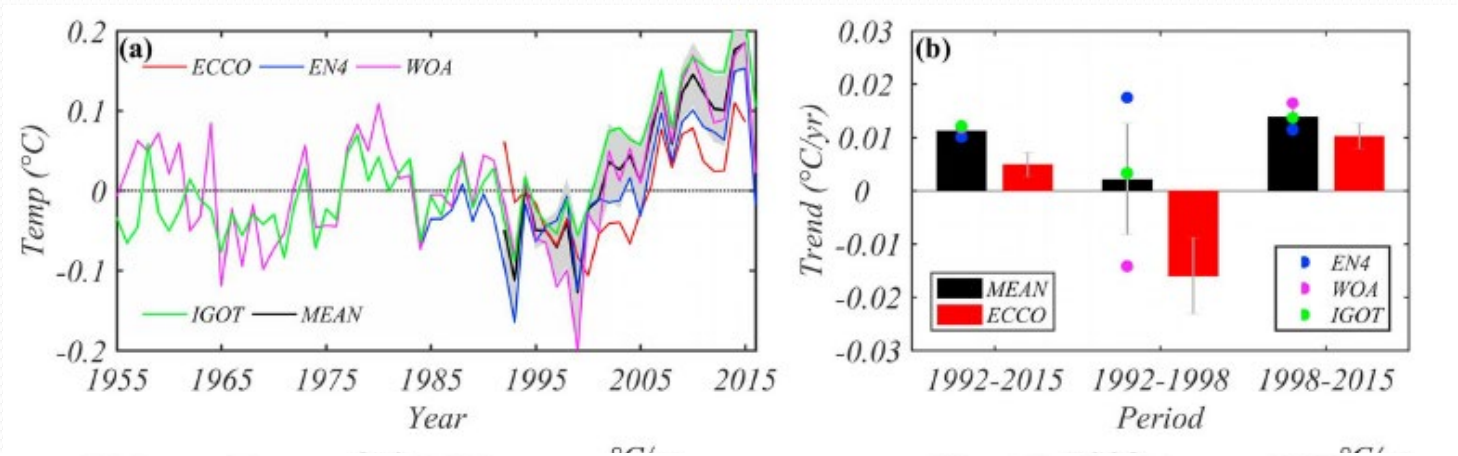


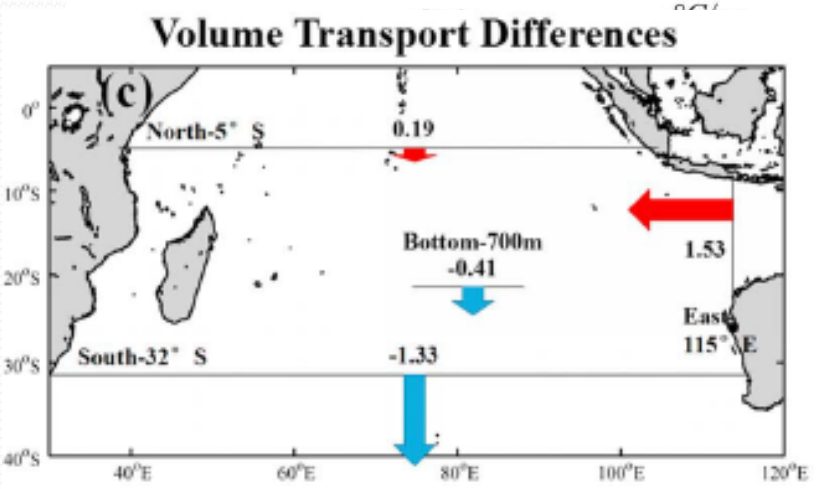


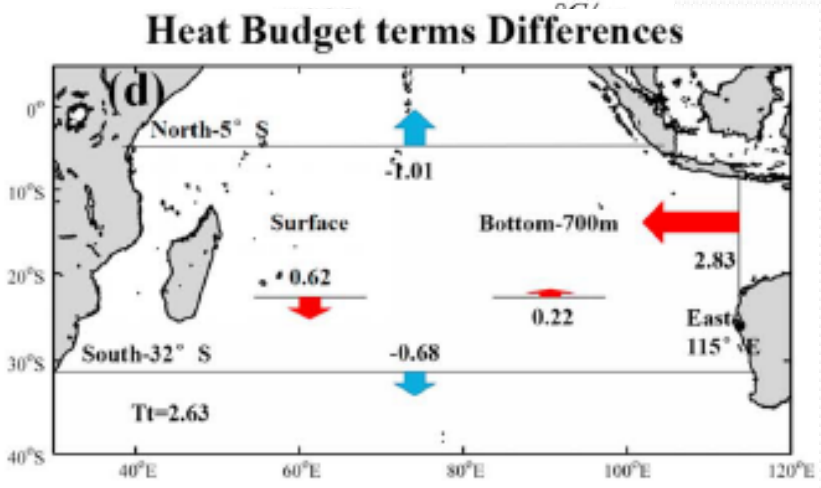


Southern tropical Indian Ocean also show similar trend for the upper 700 m water column heat content.

Zhang et al., 2018

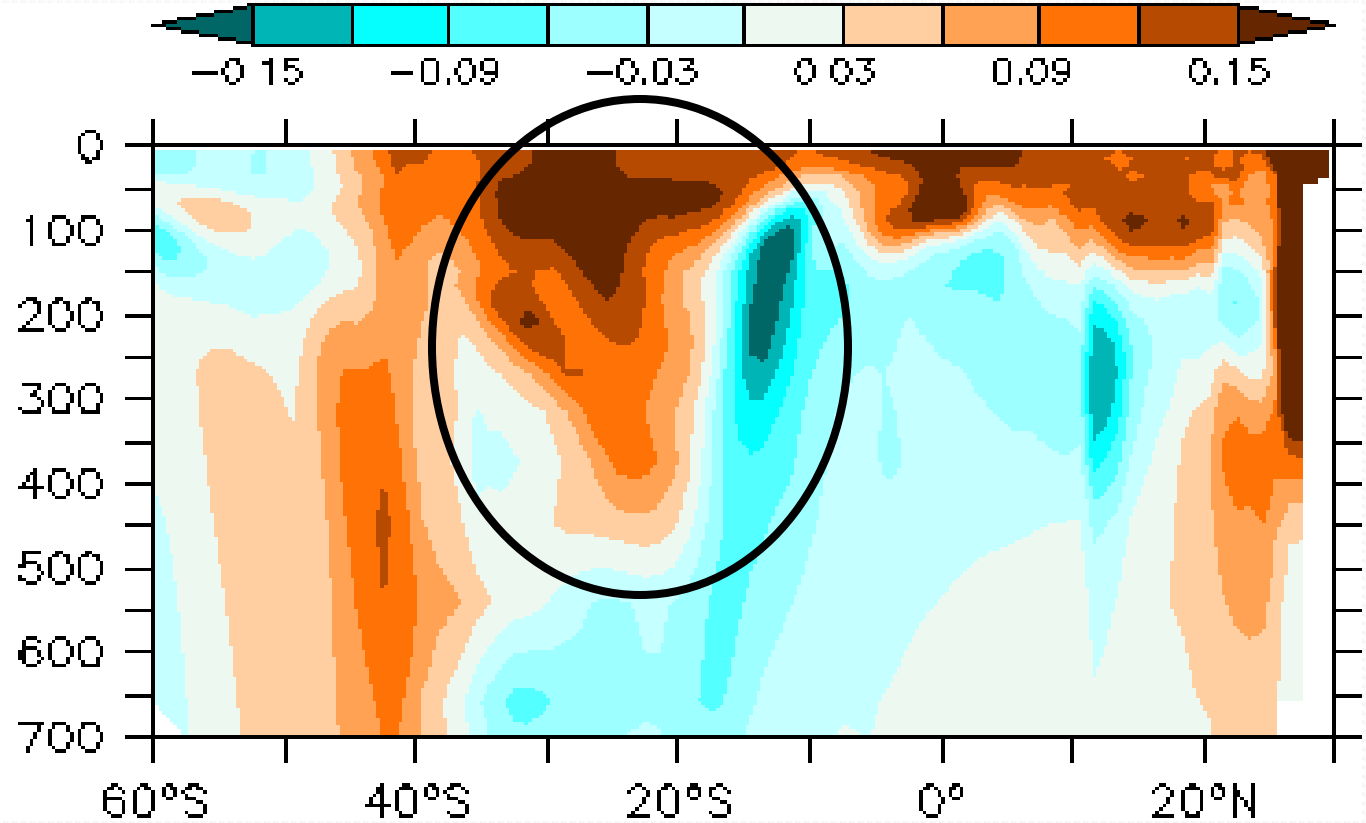


In order to understand that lets go back to the heat budget.

# Heat budget of the Indian Ocean using ORAS4

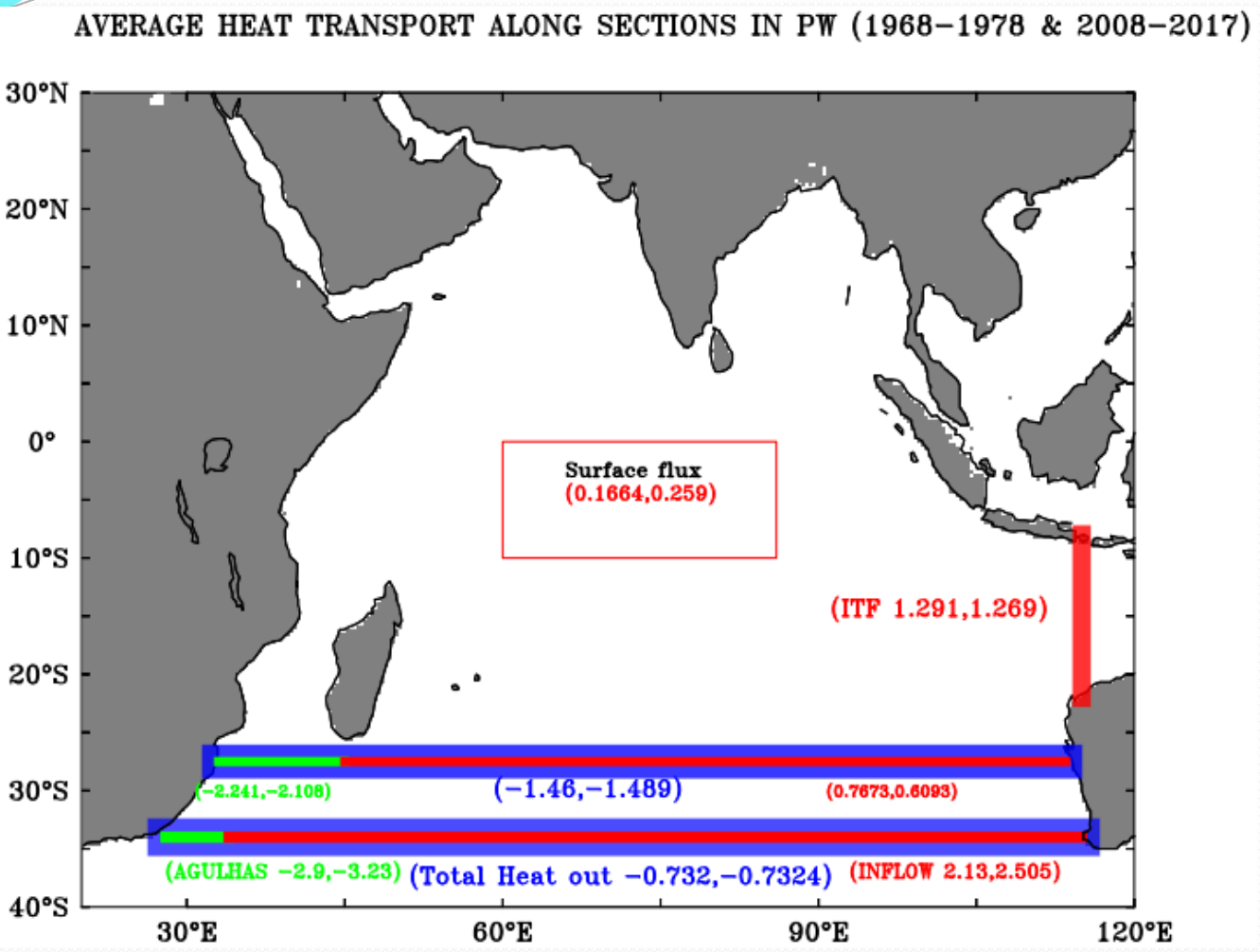


The RED sections show heat inflow and the BLUE sections Show heat outflow. The GREEN section show heat outflow through Aghulas currents.

# Heat budget of the Indian Ocean using ORAS4

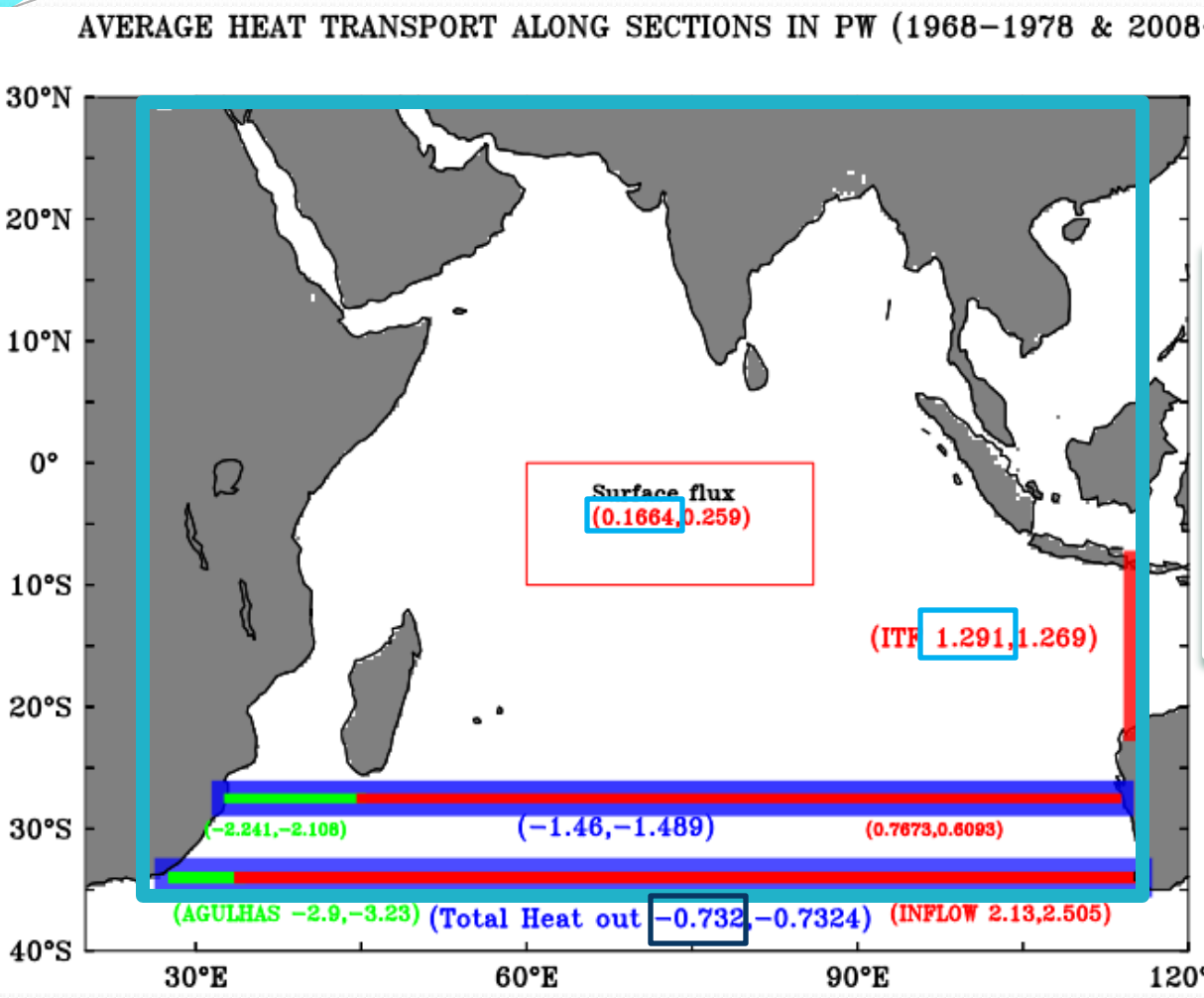


For the entire IO (34°S-30°N)

During 1968-1977 era

Total heat gain by IO =
ITF + Surf. flux – South outflow
(1.291) + (0.1664)-(0.732) PW =

0.725 PW

During 2008-2017 era

Total heat gain by IO =
ITF + Surf. flux – South outflow
(1.269) + (0.259)-(0.732) PW =

0.796 PW

The RED sections show heat inflow and the BLUE sections Show heat outflow. The GREEN section show heat outflow through Aghulas currents.

# Heat budget of the Indian Ocean using ORAS4

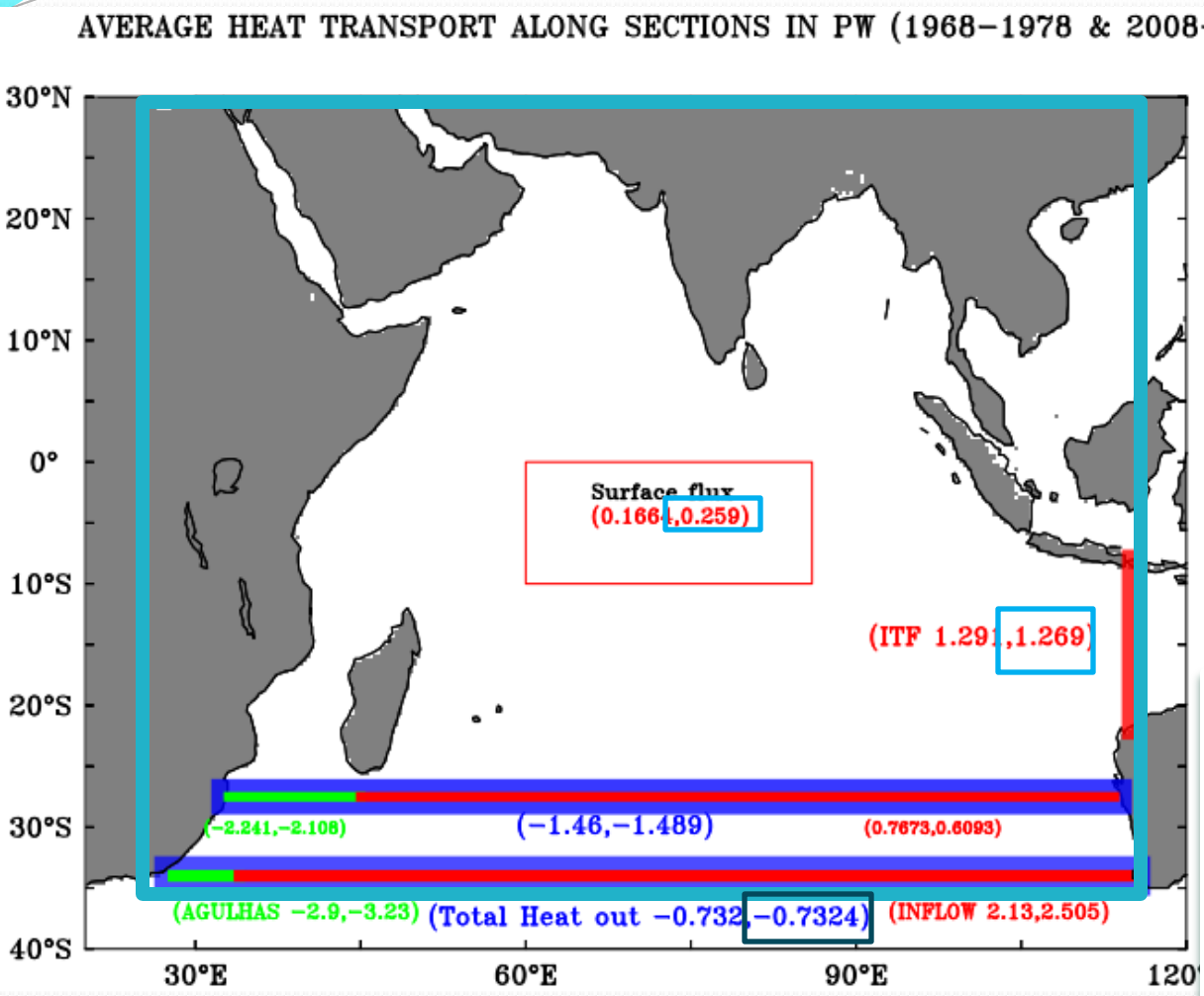


The RED sections show heat inflow and the BLUE sections Show heat outflow. The GREEN section show heat outflow through Aghulas currents.

## For the entire IO (34°S-30°N)

During 1968-1977 era

Total heat gain by IO =
ITF + Surf. flux – South outflow
(1.291) + (0.1664)-(0.732) PW =

**0.725 PW**

During 2008-2017 era

Total heat gain by IO =
ITF + Surf. flux – South outflow
(1.269) + (0.259)-(0.732) PW =

**0.796 PW**

# Heat budget of the Indian Ocean using ORAS4

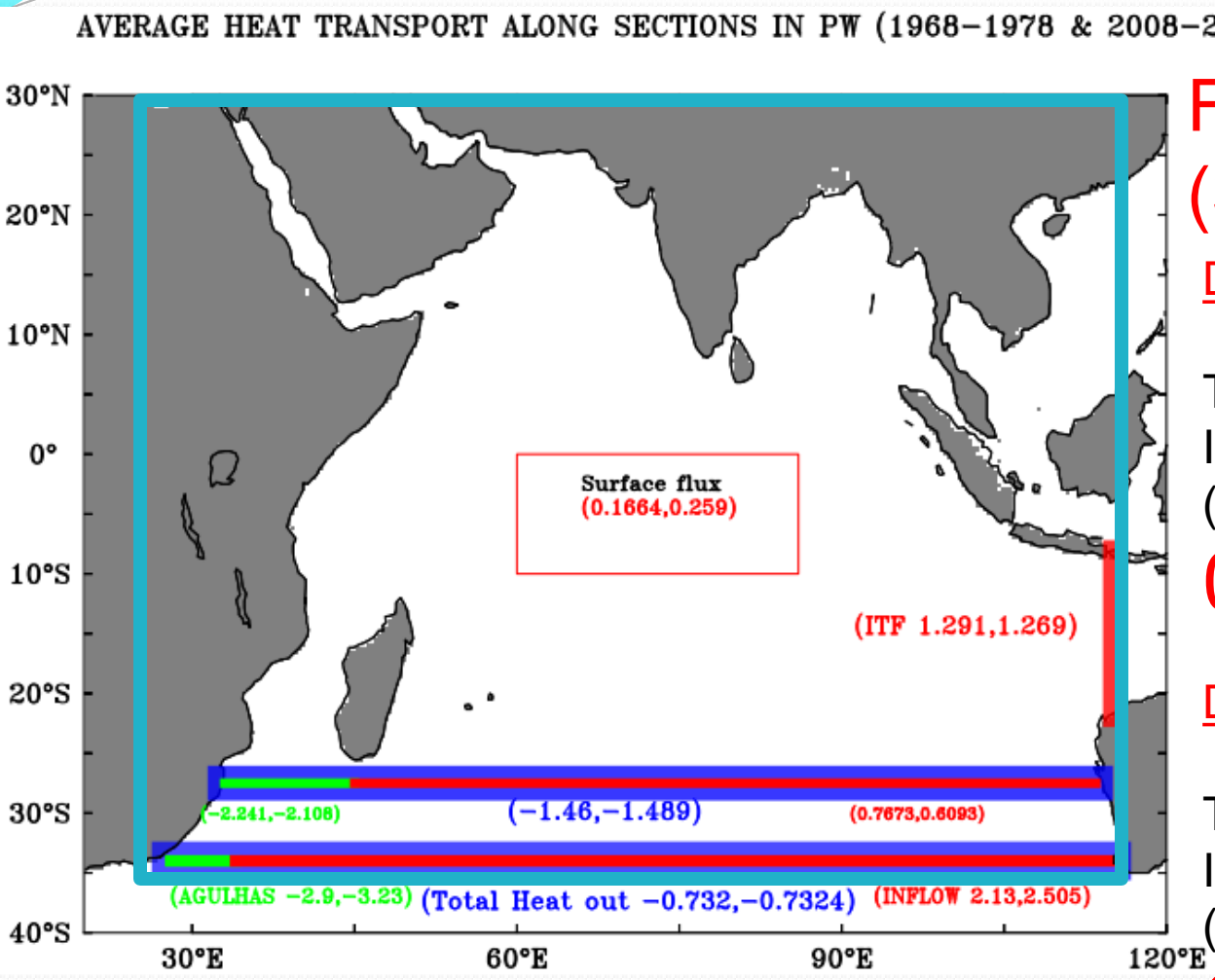


For the entire IO (34°S-30°N)

During 1968-1977 era

Total heat gain by IO =
ITF + Surf. flux – South outflow
(1.291) + (0.1664)-(0.732) PW =

0.725 PW

During 2008-2017 era

Total heat gain by IO =
ITF + Surf. flux – South outflow
(1.269) + (0.259)-(0.732) PW =

0.796 PW

**During the last 40 years net heat flux to the IO has increase by** $7 \times 10^{14}$ J/sec

# Heat budget of the Indian Ocean using ORAS4

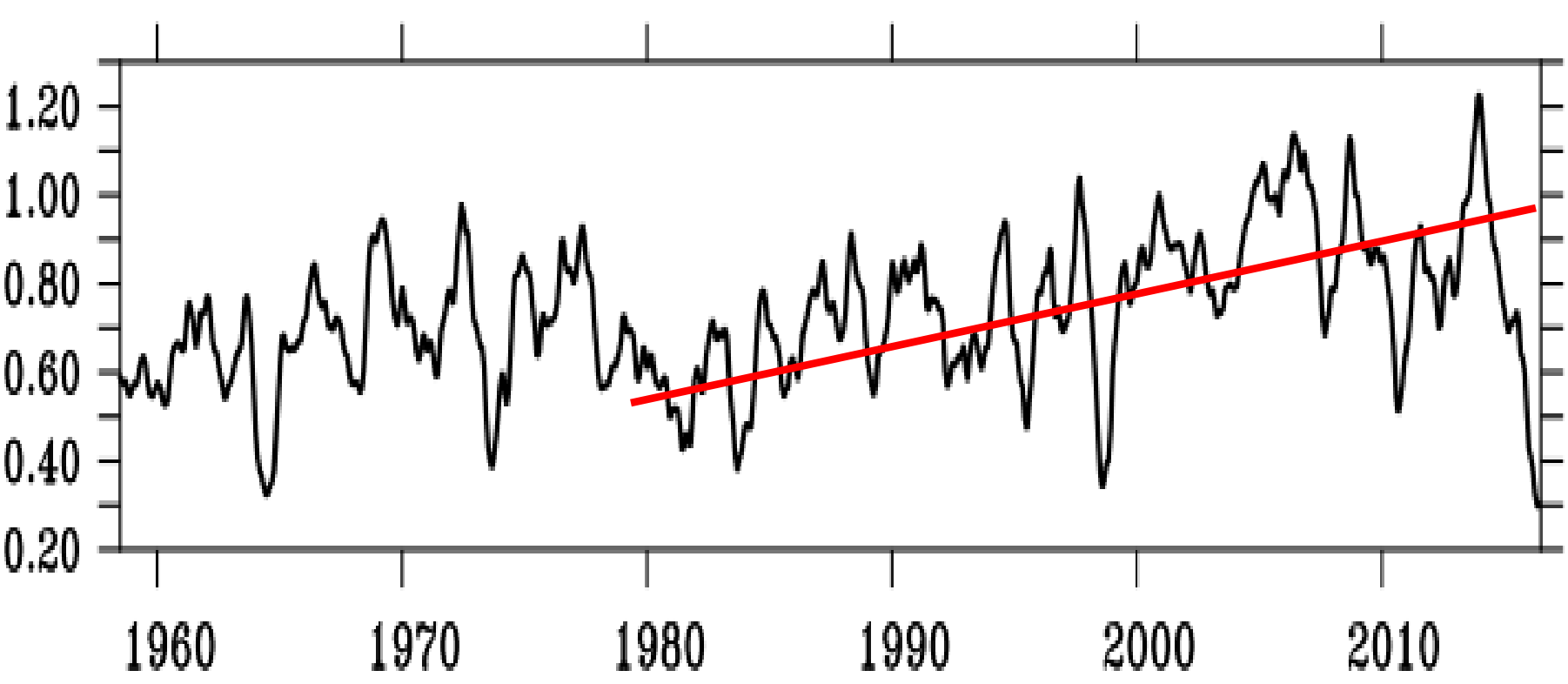


Total net heat flux (PW) into the IO is always positive, but the rate has increased rapidly since the post industrial era. The increase in heat flux is much prominent in the south-eastern section off Australia.

# Why south IO warming is more intense

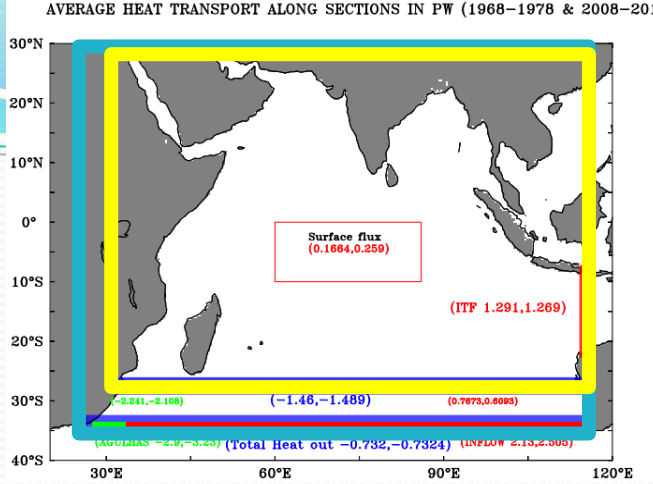


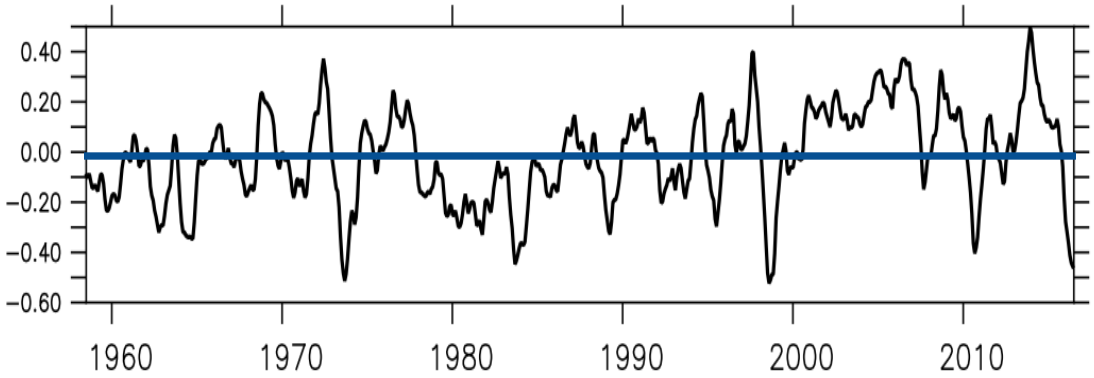


Net heat flux for the YELLOW BOX (27°S).
There is no net gain by the YELLOW basin except in the recent decade.

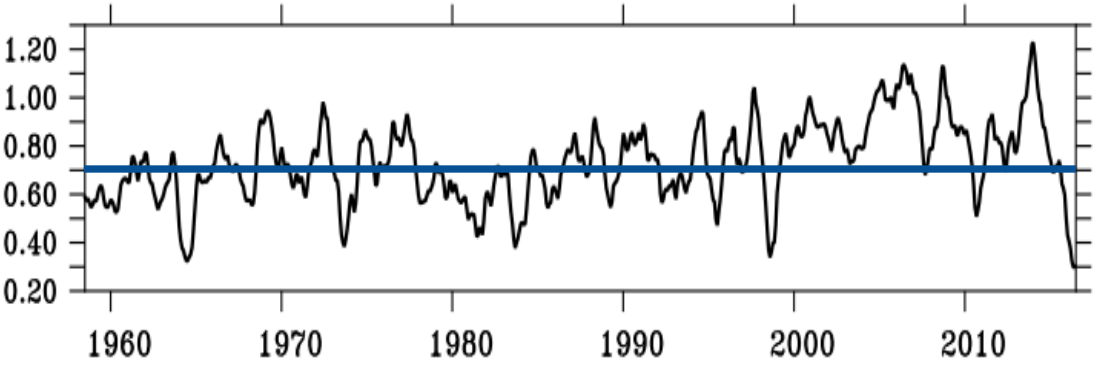


Net heat flux for the CIYAN BOX (34°S).
There is a net gain by the CIYAN basin of the order of 7 x $10^{14}$ J/s.

# Why south IO warming is more intense

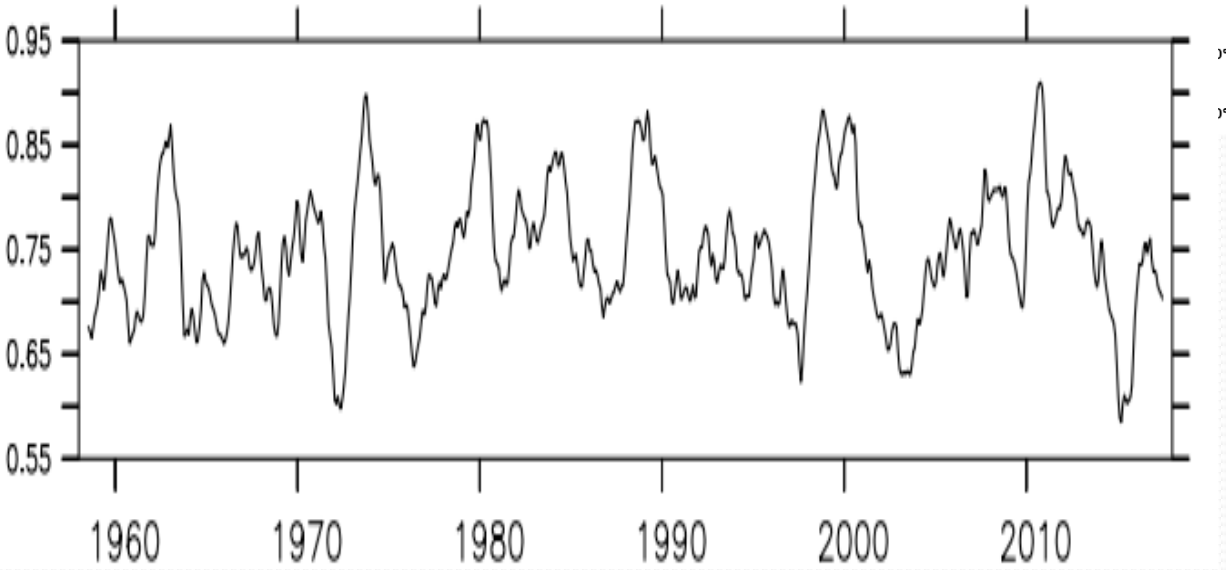


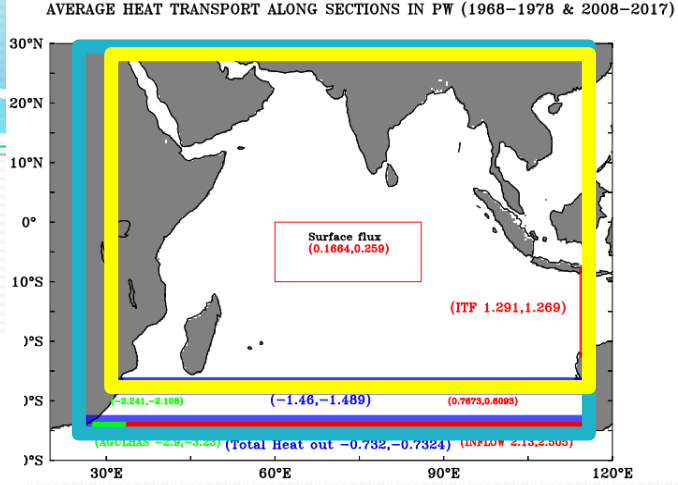


Difference between the net heat flux between CYAN BOX (34°S) and YELLOW BOX (27°S)

The average heat gain by the 27-34°S band is $7 \times 10^{14}$ J/s which is equivalent to the total heat gain by the IO. This suggest that most of the heat gets trapped within this band resulting a much stronger heating of this region.

Trend of the thermocline (D20; left) and SSH (middle) from ORAS4. The right panel showing a comparison between time series of averaged (over black box) field of D20 (left axis) and SSH (right axis).

Figure 4

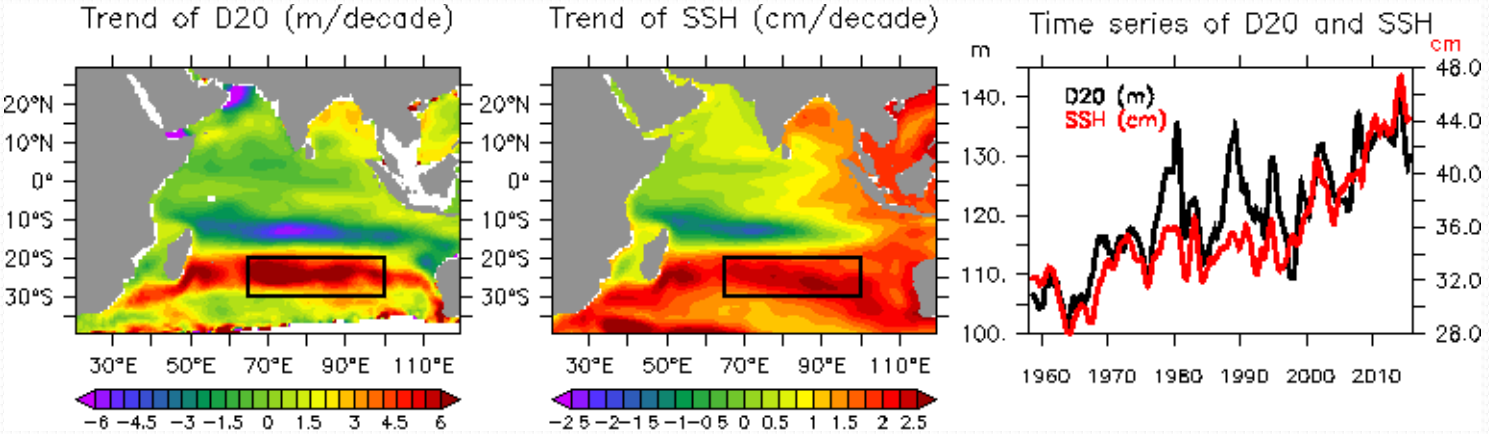


D20 is deepening by ~4-5 m/decade in the south IO over the 20-30°S latitude belt. Note that SSH also show a similar increasing trend over the same period. Interestingly, a box averaged (65-100°E/20-30°S) comparison of these two variable show very similar variability since 1958 (starting date of ORAS4).

This indicates that the variability of SSH and D20 is most likely linked to each other and thus driven by propagating waves or local Ekman pumping. Advection of heat through ITF looks unlikely.

Note that this deepening of thermocline not only increase SSH, but also shows up in the warming trend of subsurface temperature of this region.

# Role of local Ekman pumping

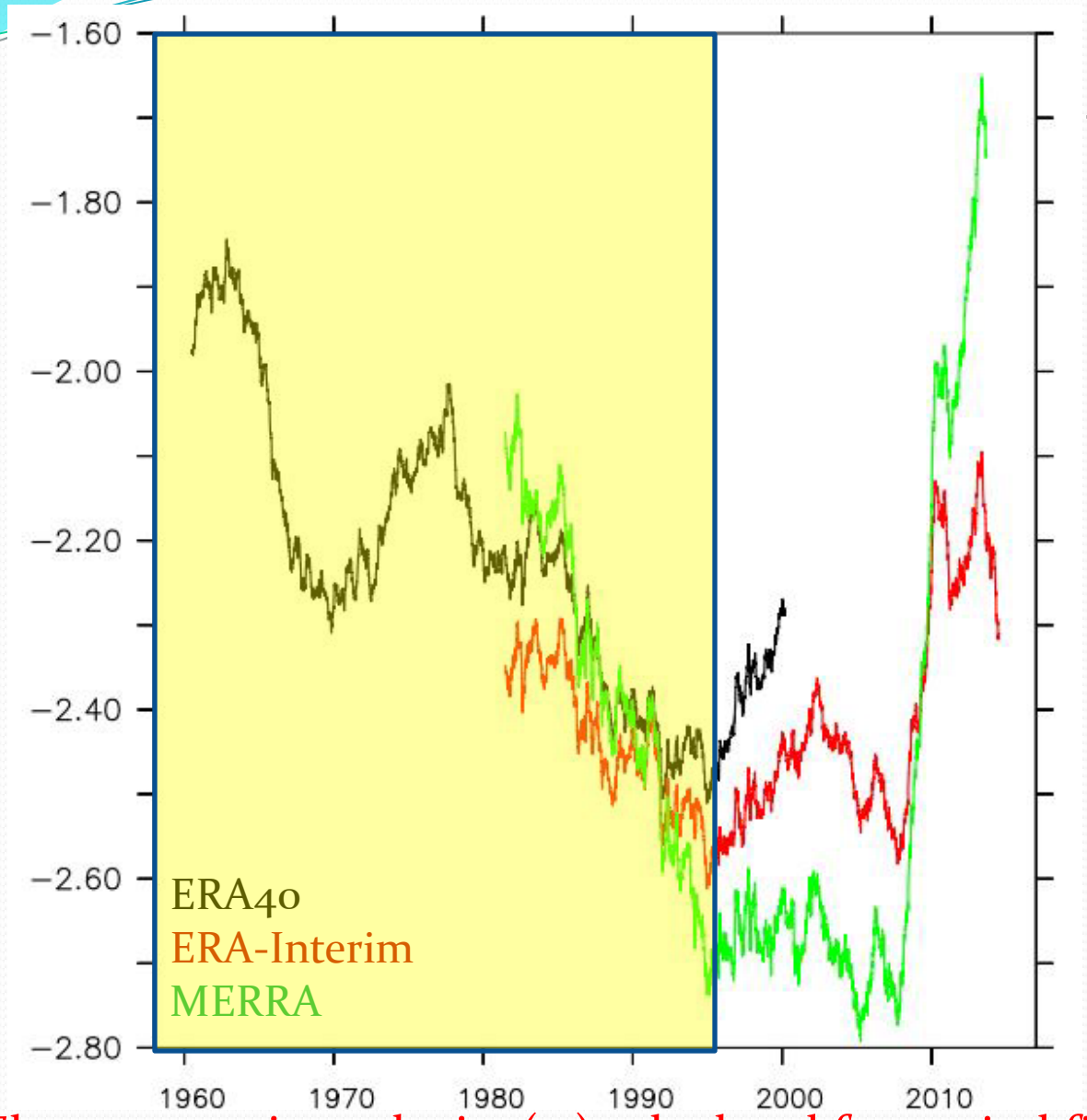


Ekman pumping velocity is favorable for deepening of thermocline till 1990's. Indicating that most of the heat converged into the 20-30°S owing to the wind driven local Ekman pumping. This also resulted in increasing trend of SSH.

However, Ekman pumping decreases in recent decade opposed to the increasing trend of SSH and D20.

Ekman pumping velocity (w) calculated from wind fields over 90-100E/20-30S

# Role of Rossby waves

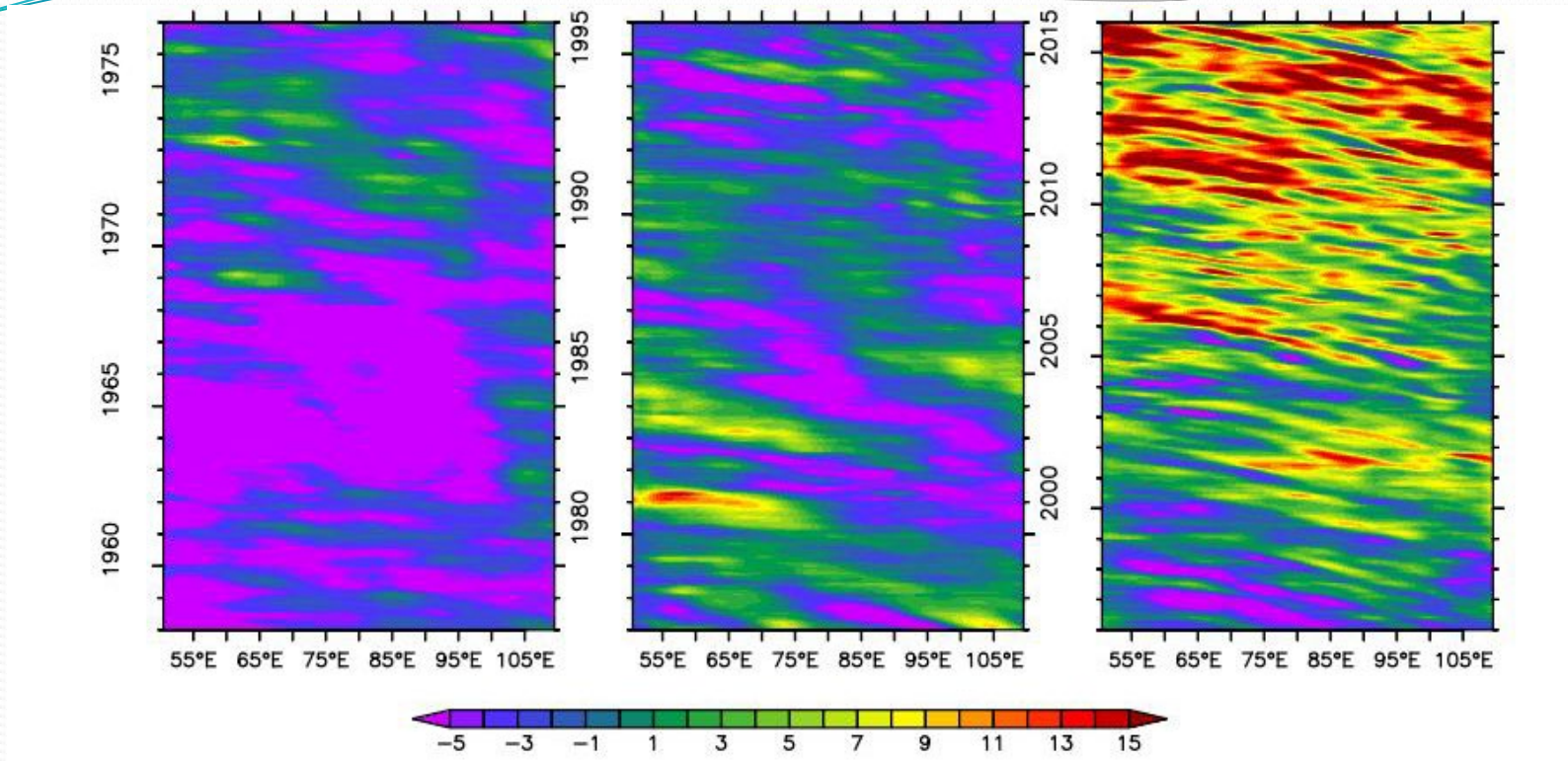


Hovmoller diagram of SSH (annual signal removed) along the $25^0$S latitude belt indicates that downwelling favorable Rossby waves intensified rapidly post 1995. The westward propagation is much prominent during recent decade.

This suggests that post 1995 deepening of the thermocline in the 20-30$^o$S is driven primarily by remotely forced Rossby waves and thereby converges heat in this band.

What drives these Rossby waves and where?

# Rossby waves are generated south of Australia and brings heat into the Indian Ocean through southern boundary

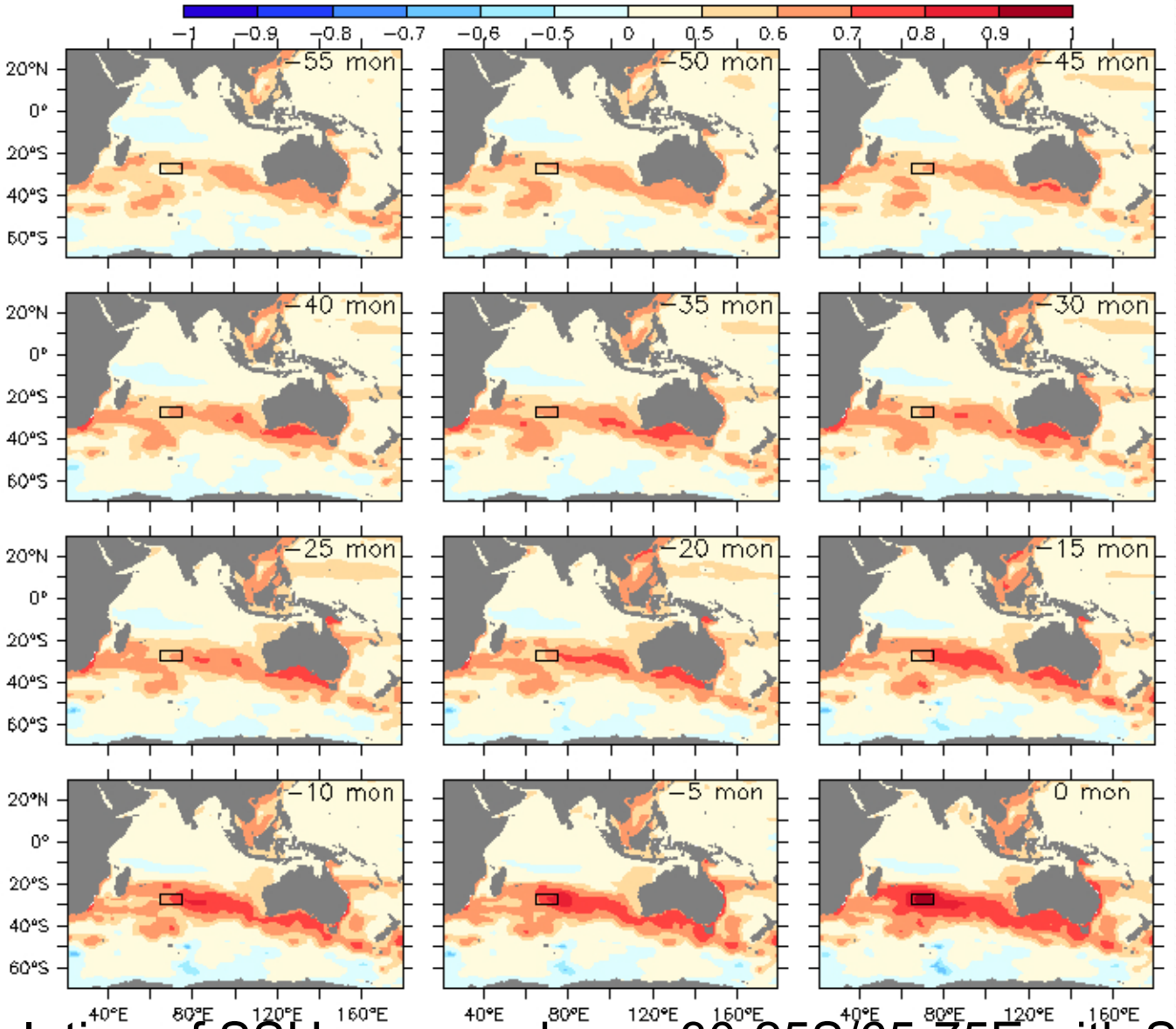


Lag correlation of SSH averaged over 30-25S/65-75E with SSH of the rest of the globe.

# What drives this Rossby waves?

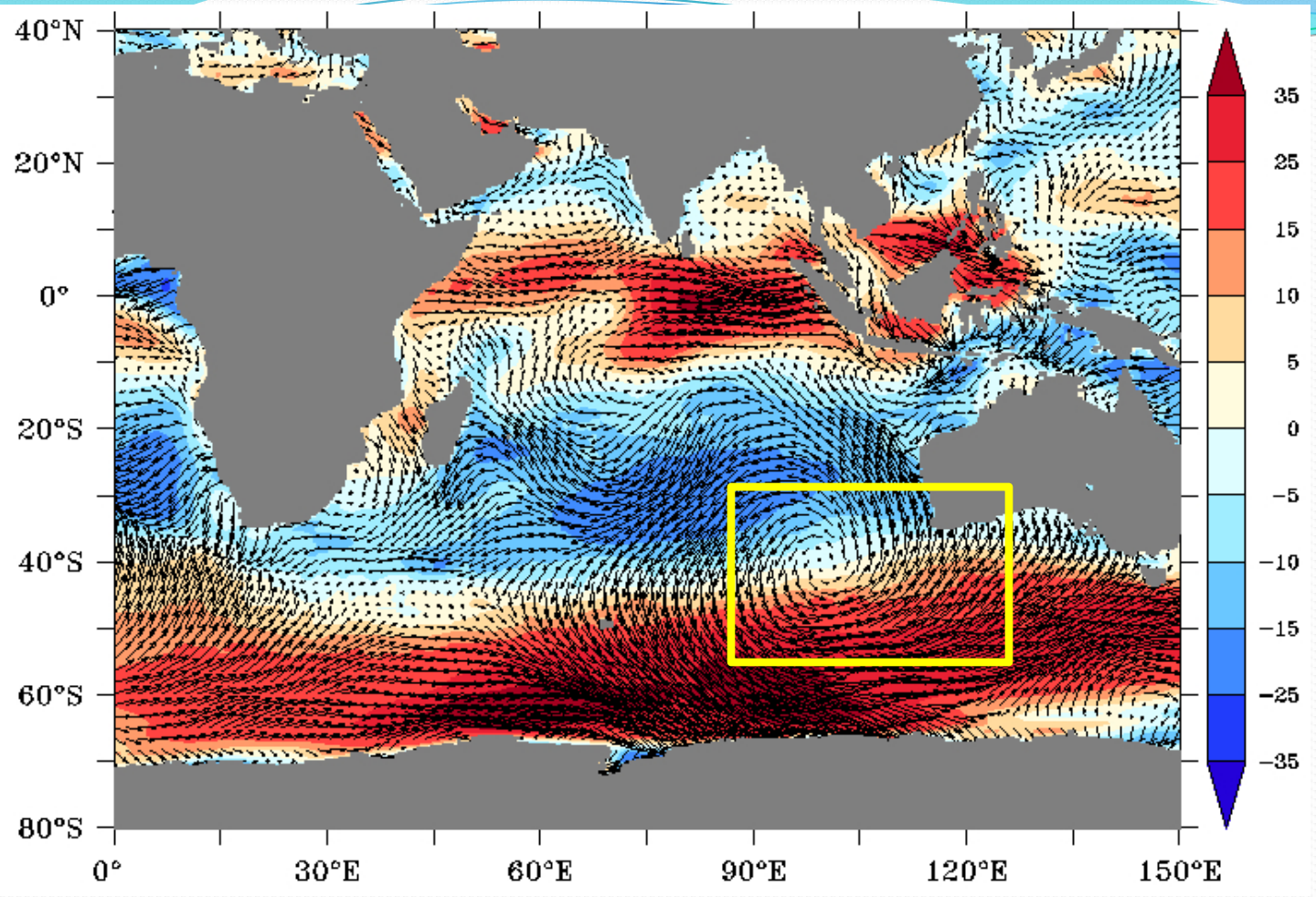


Wind speed trend (shaded) and trend of U10 and v10 plotted as vector. Trend is calculated for 1979-2017 using JRA55-do atmospheric fields.

Recent decades witnessed an warming trend in the southern Ocean. This resulted in enhanced pressure gradient between polar low and extatropical high which increases the strength of the easterlies in the extra tropics. This enhanced easterlies lead to a stronger positive wind curl south of Australia and therefore, radiate downwelling Rossby waves into the Indian Ocean.

# Role of internal variability in the decadal variability of the south tropical Indian Ocean?

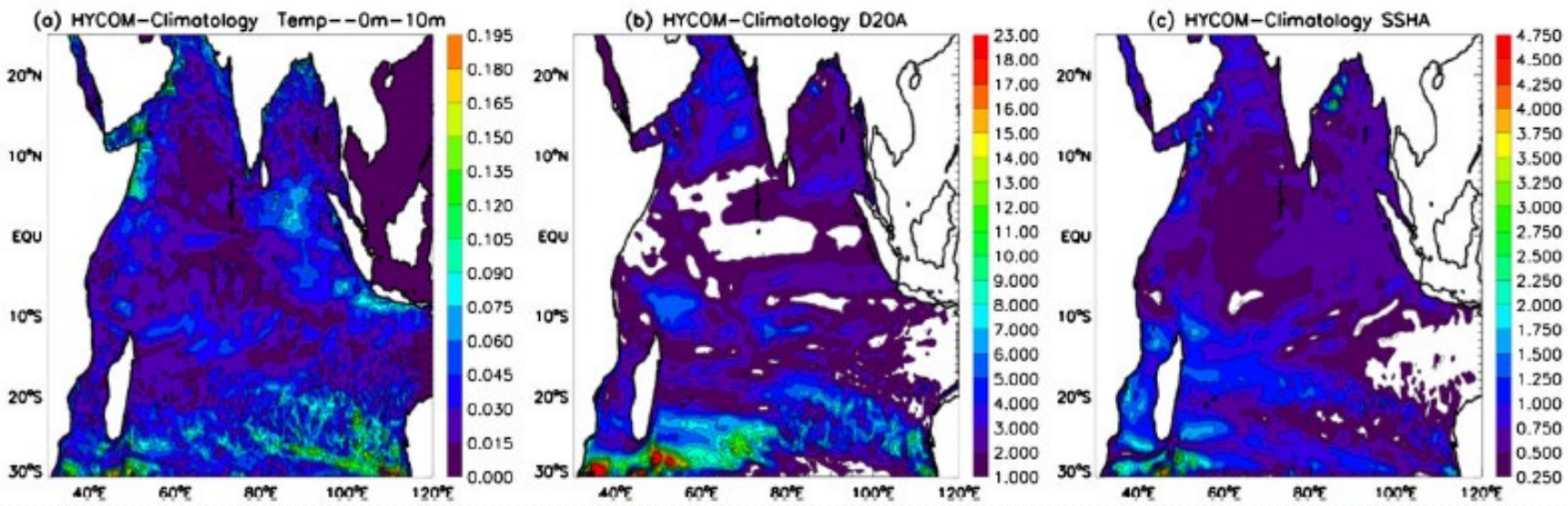


Trenary and Han, 2013

# Climate modelling

**Objectives:**

Assess the impact of climate change on Indian Ocean warming, sea level change and marine biogeochemistry.

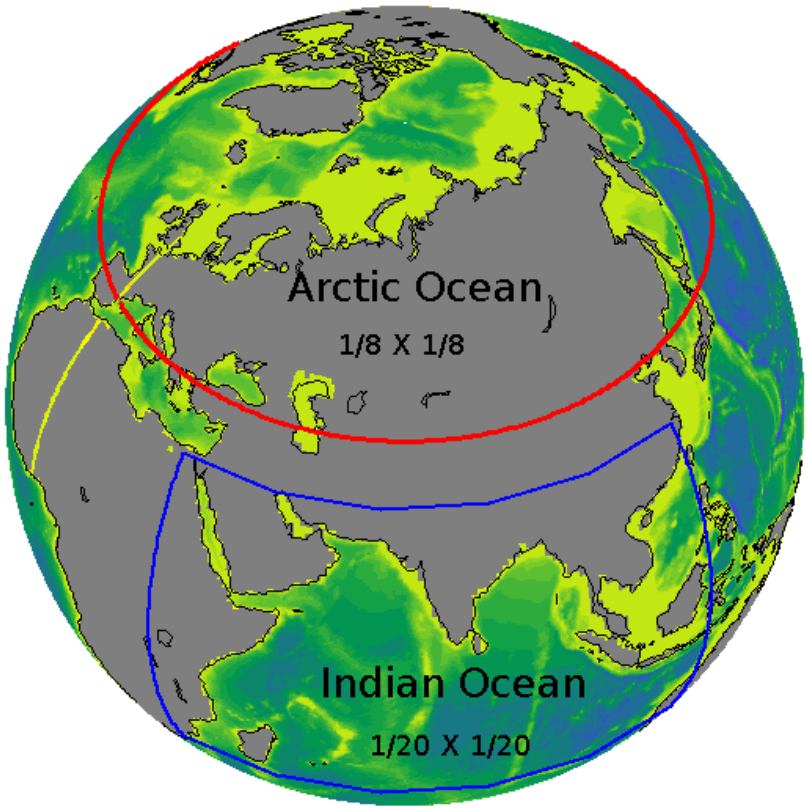


**Configurations:**

In order to resolve the spatial and temporal scale three configurations are planned:

(a) Global model (1/8°X18°; 5 m vertical resolution in top 50 m and total 42 levels).

(b) Indian Ocean model (1/20°X20°; ~1-1.5 m vertical resolution in top 30 m and total 50 levels).

(c) Arctic Ocean model (1/8°X18°; 5 m vertical resolution in top 50 m and total 50 levels) .

# Model produces IO subsurface warming trend and climate modes reasonably well.

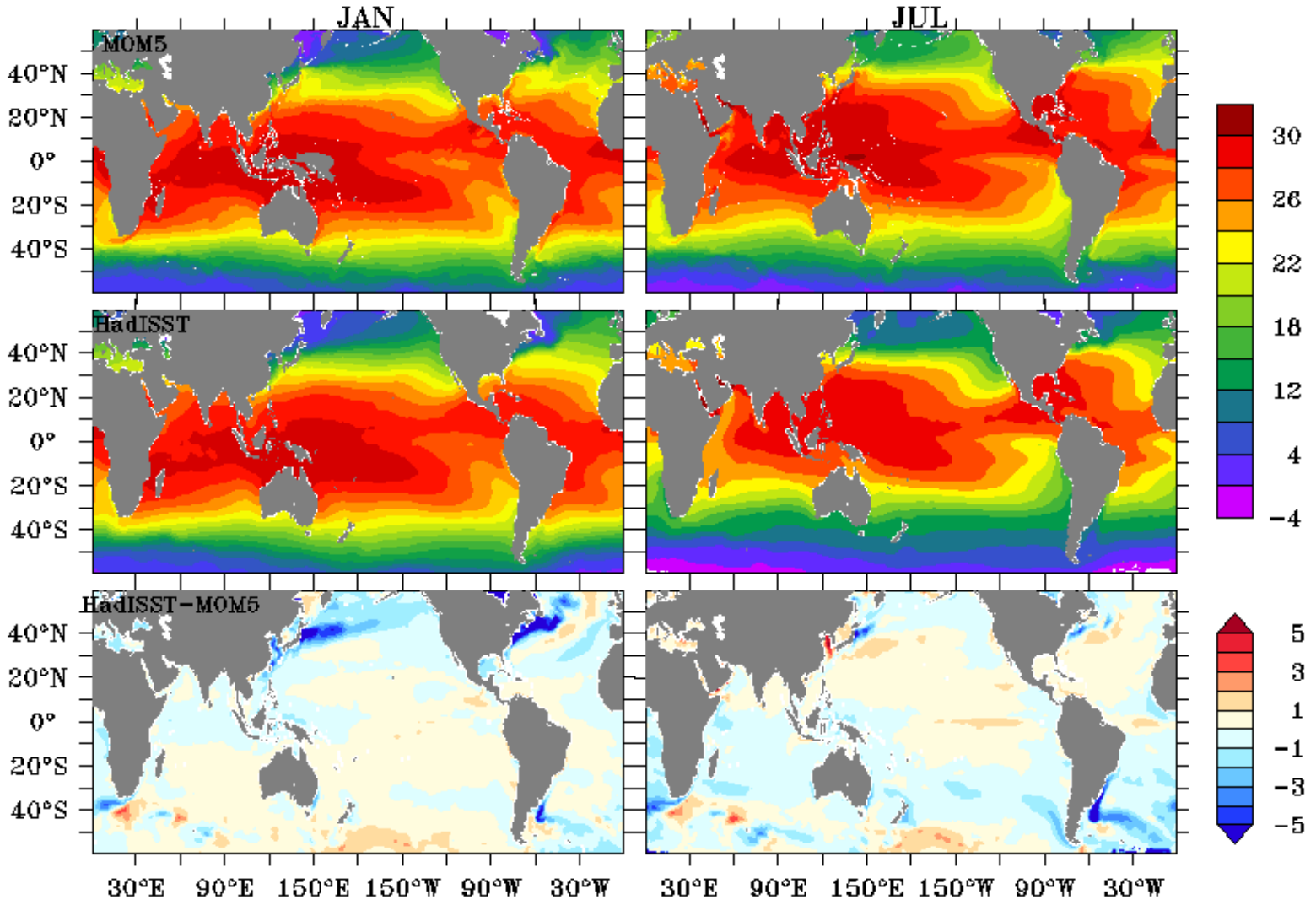


Comparison of monthly climatological SST map for January and July for 1962-2014.

# Model produces IO subsurface warming trend and climate modes reasonably well.

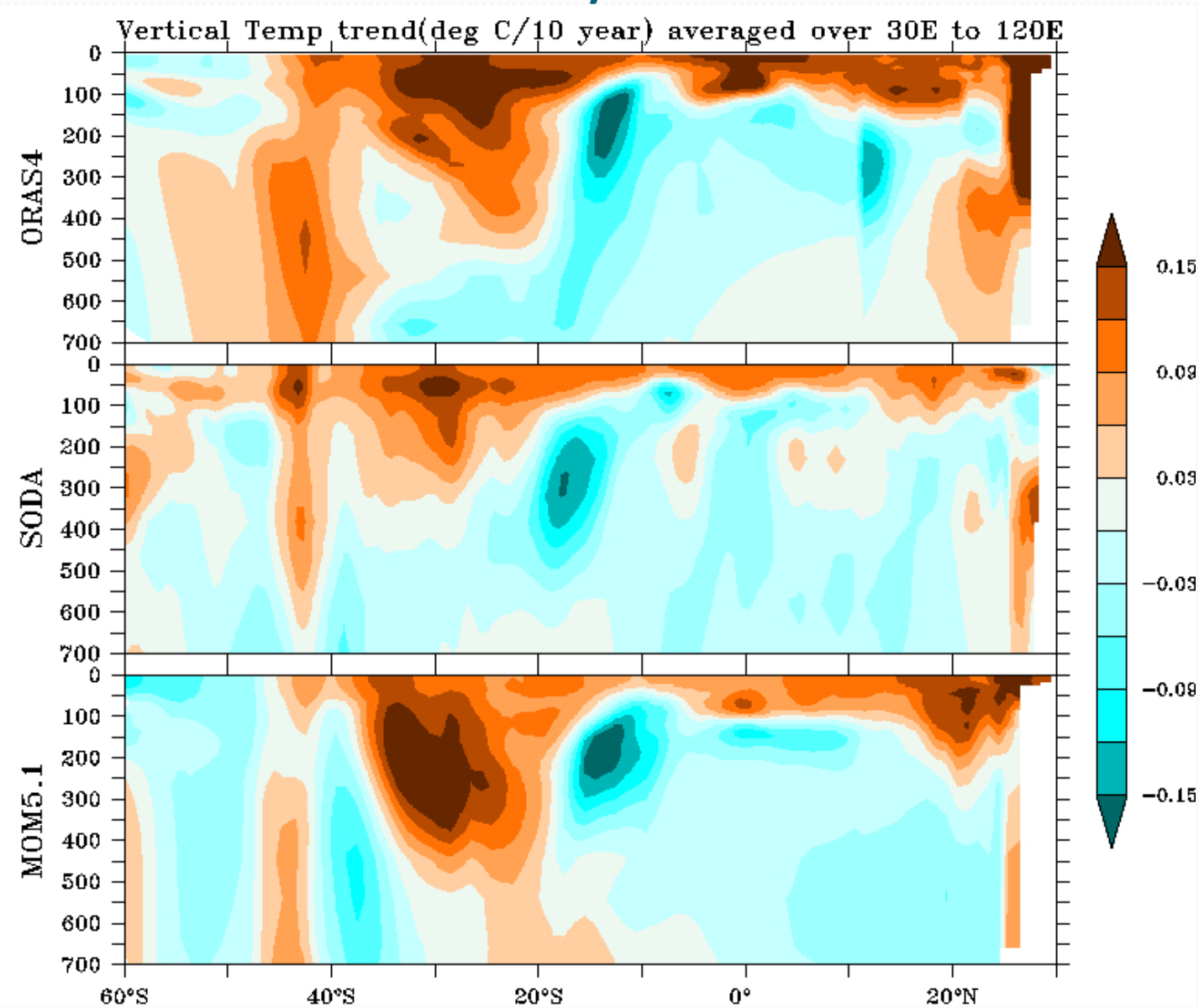

# Model produces IO subsurface warming trend and climate modes reasonably well.

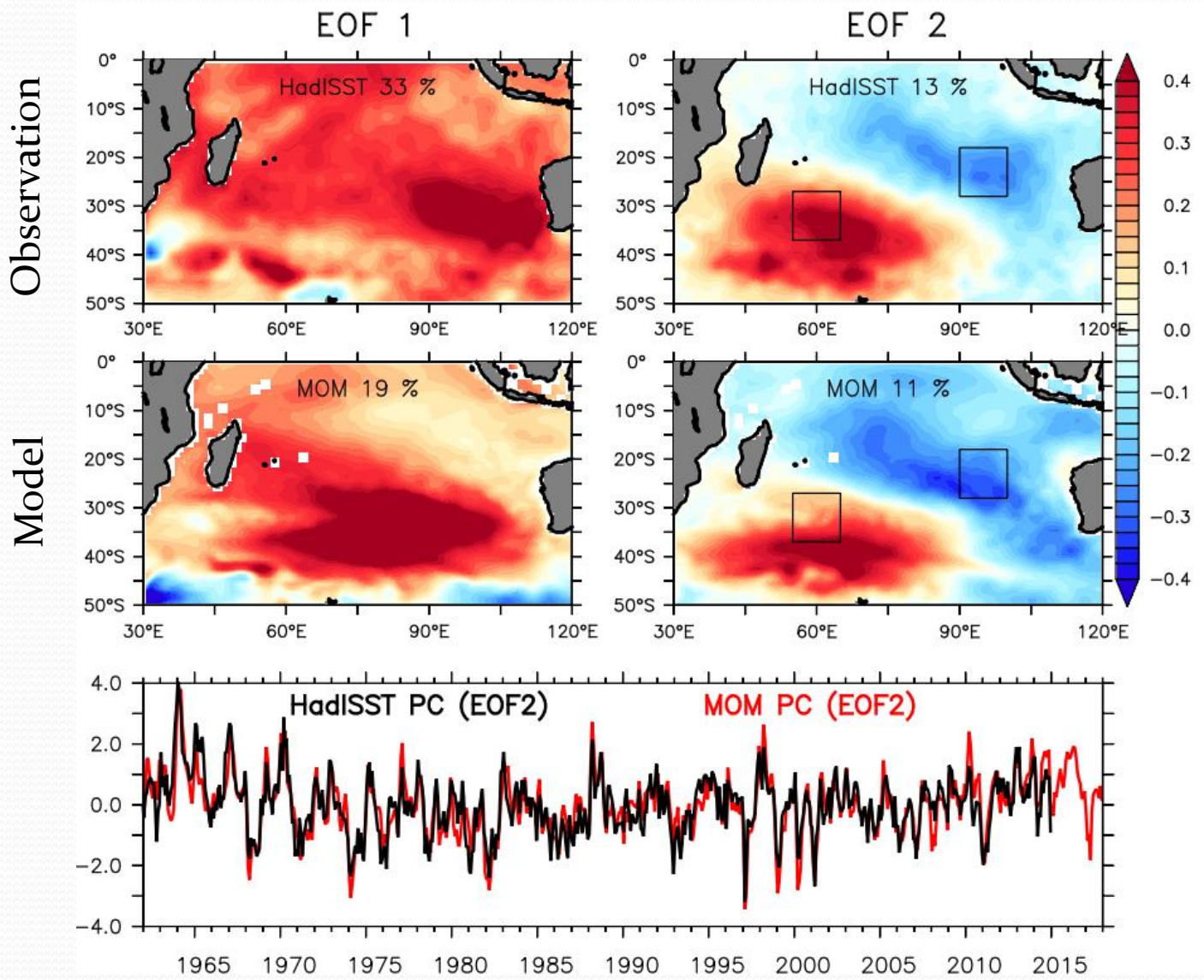

# Comparison of Subtropical Indian Ocean Dipole Mode (SIOD) between observation and model.

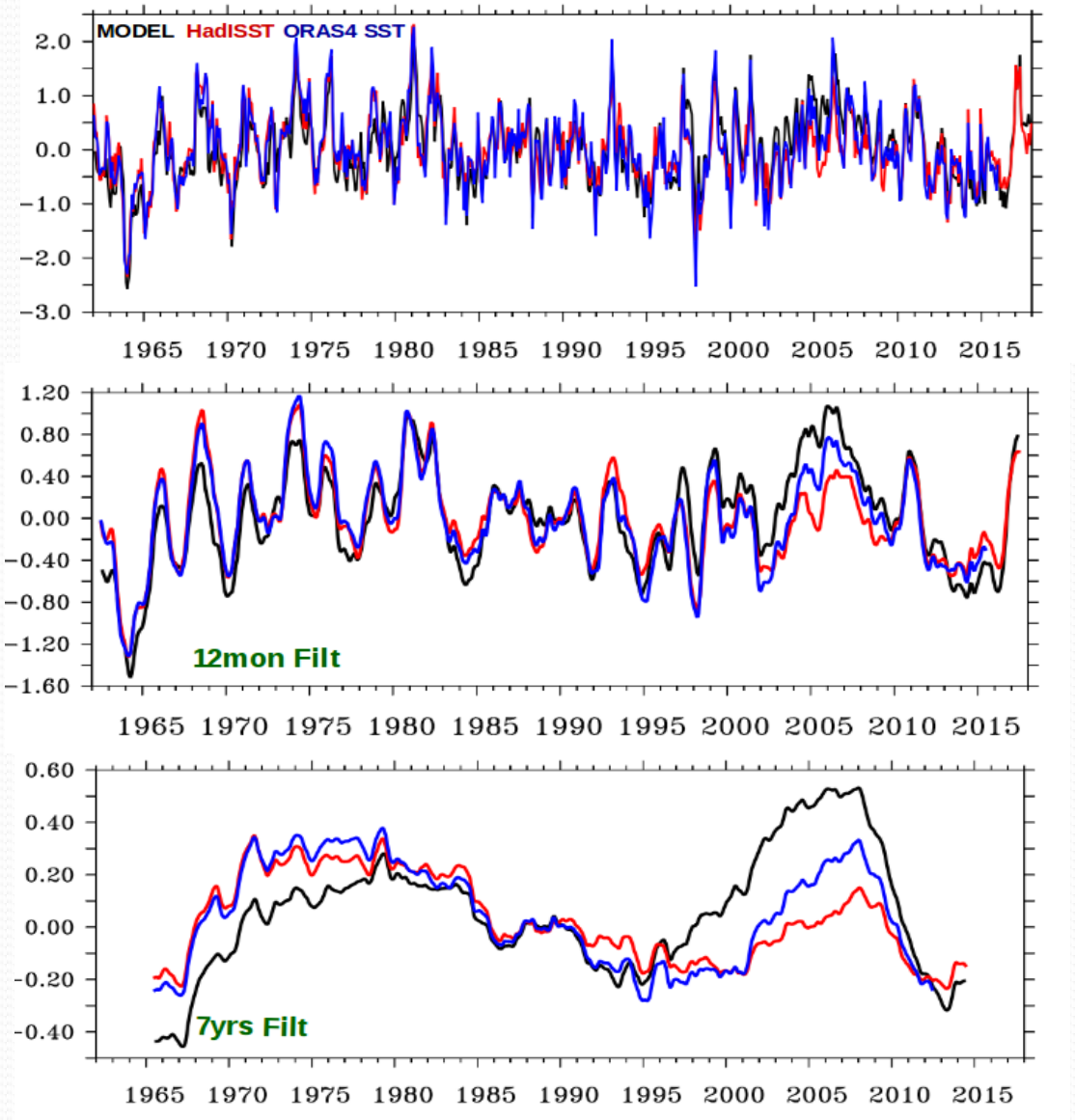


The Subtropical Indian Ocean Dipole Index is computed from SST anomaly difference between western (55-65°E,37-27°S) and eastern (90°E-100°E,28-18°S) box of the Indian Ocean.

# Comparison of SD of model simulated SST for interannual and climatological simulation

Control Run | Climatological Run

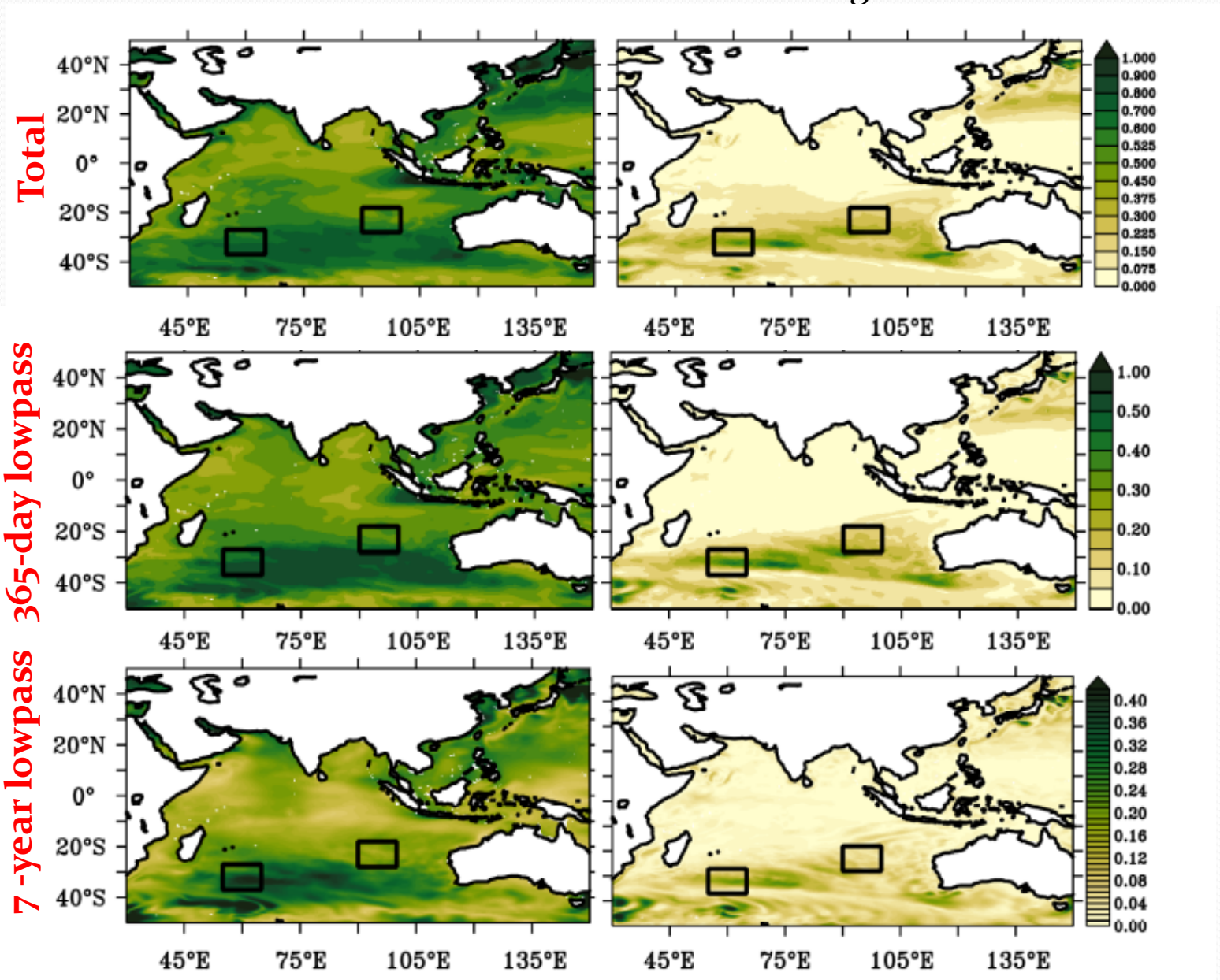

# Comparison of SD of model simulated SST for interannual and climatological simulation

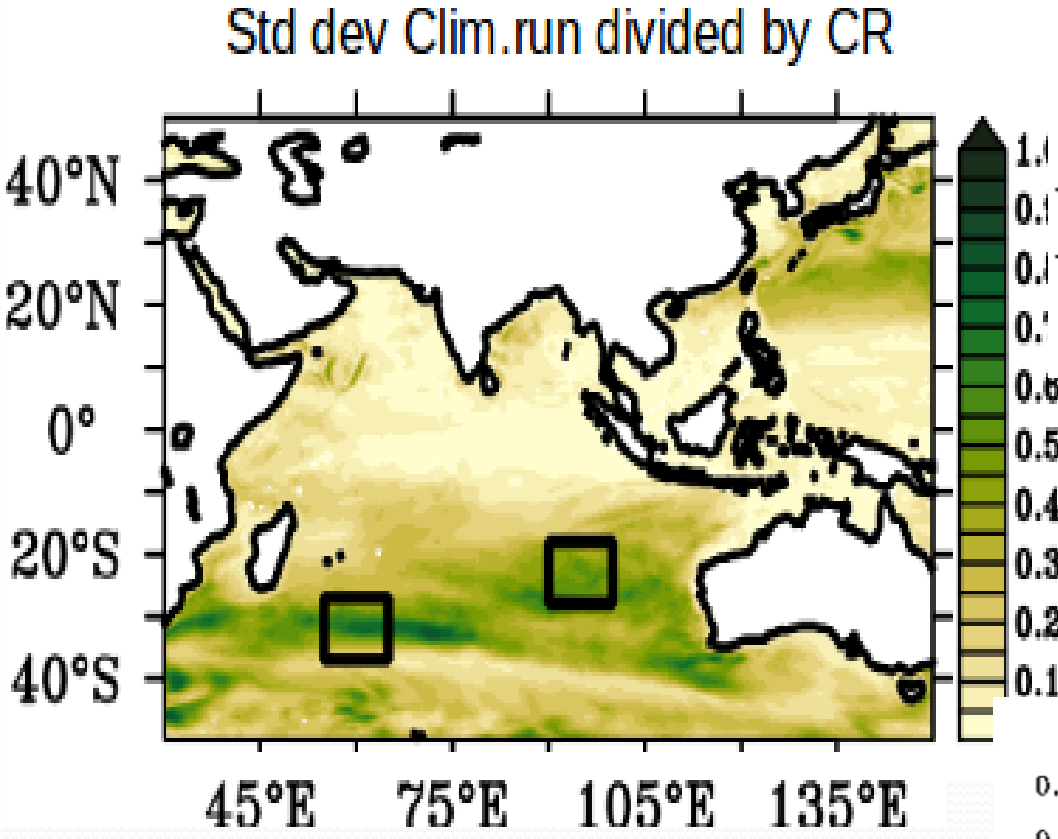


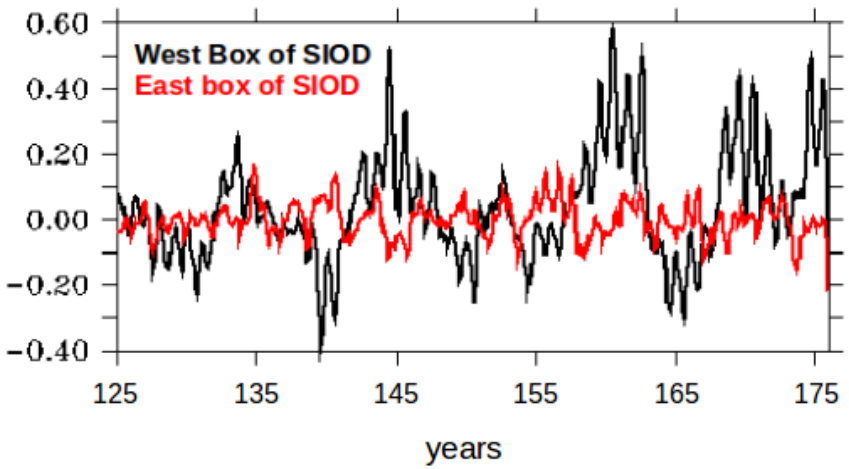


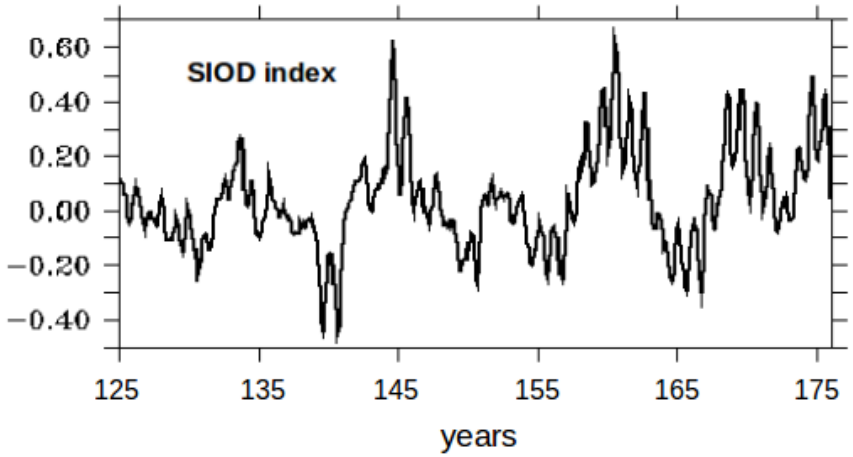


Ratio of the SDs of SST between climatological simulation and interannual simulation.

# Mechanisms for the generation of large internal variability in this region.

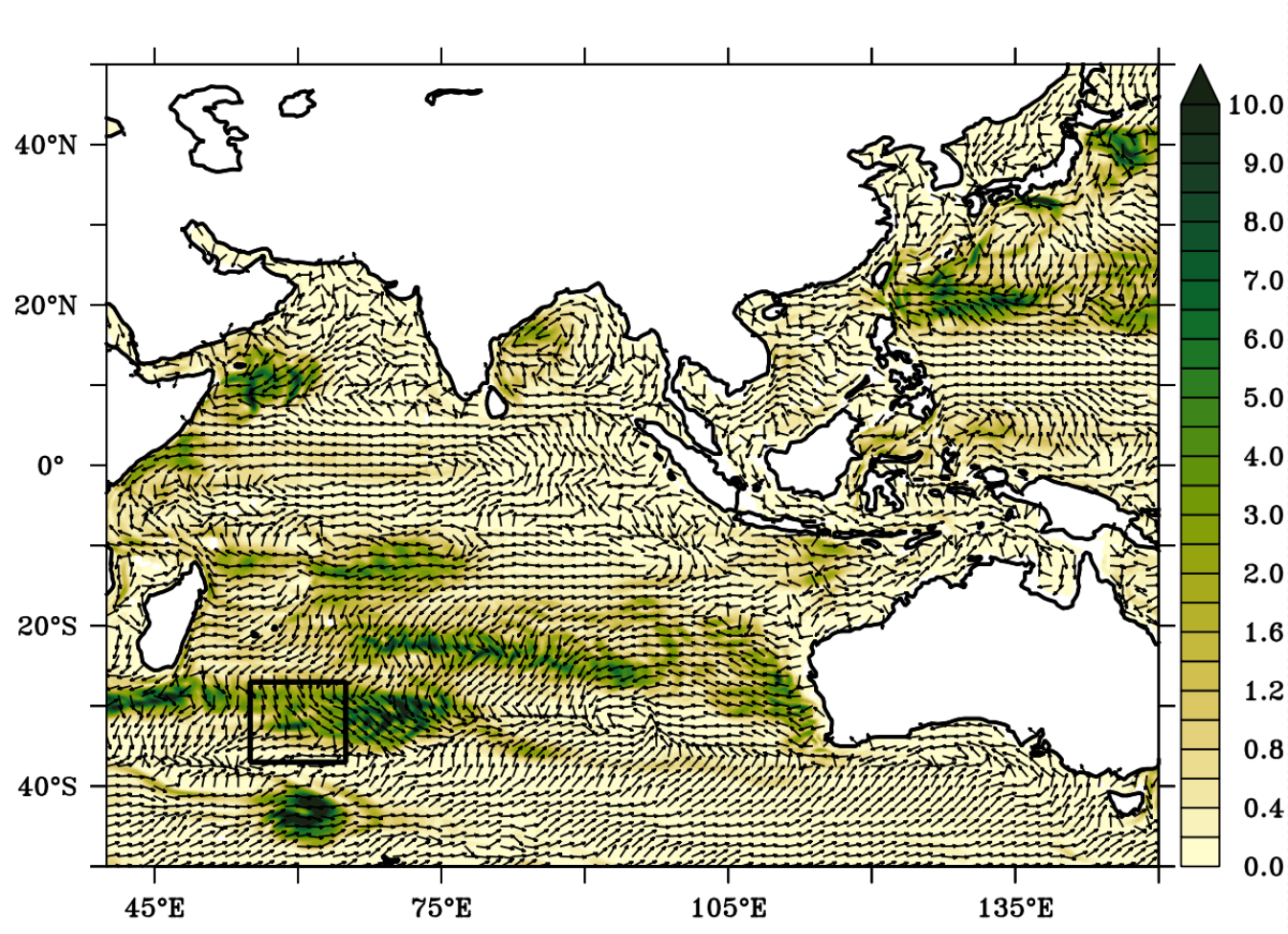


KE from of the CLIM solution using surface currents (annual cycle removed) and averaged over the final year of climatological simulation.

# Mechanisms for the generation of large internal variability in this region.

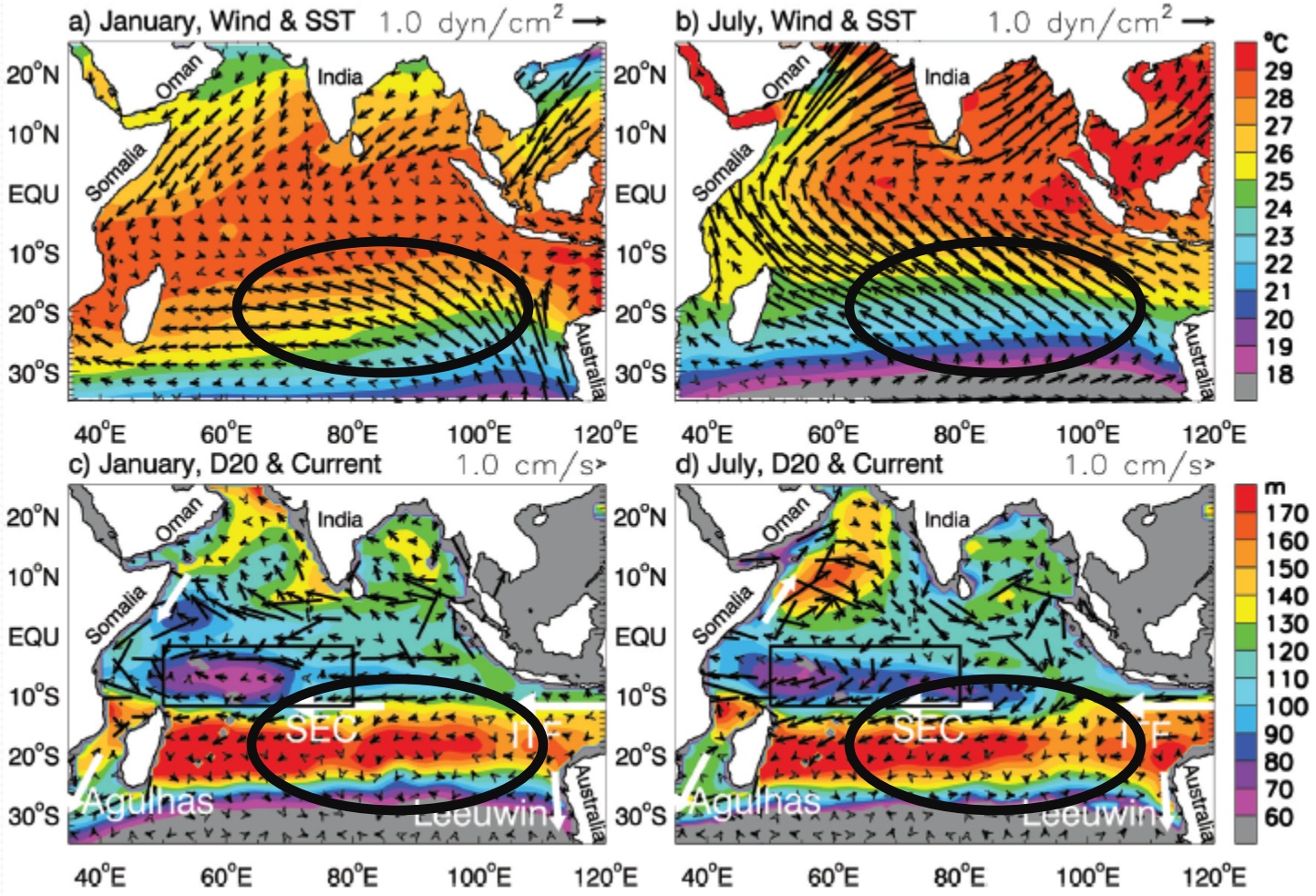


(a,b) Climatological surface maps of SST (HadISST) and winds (ECWMF) for 1960-2009, (c,d) D20 (Hosoda et al., 2008) and currents (OSCAR).

Han et al., 2014

Sea Surface Temperature from INCOIS Global Model (MOM5.1)

January 01, 2017

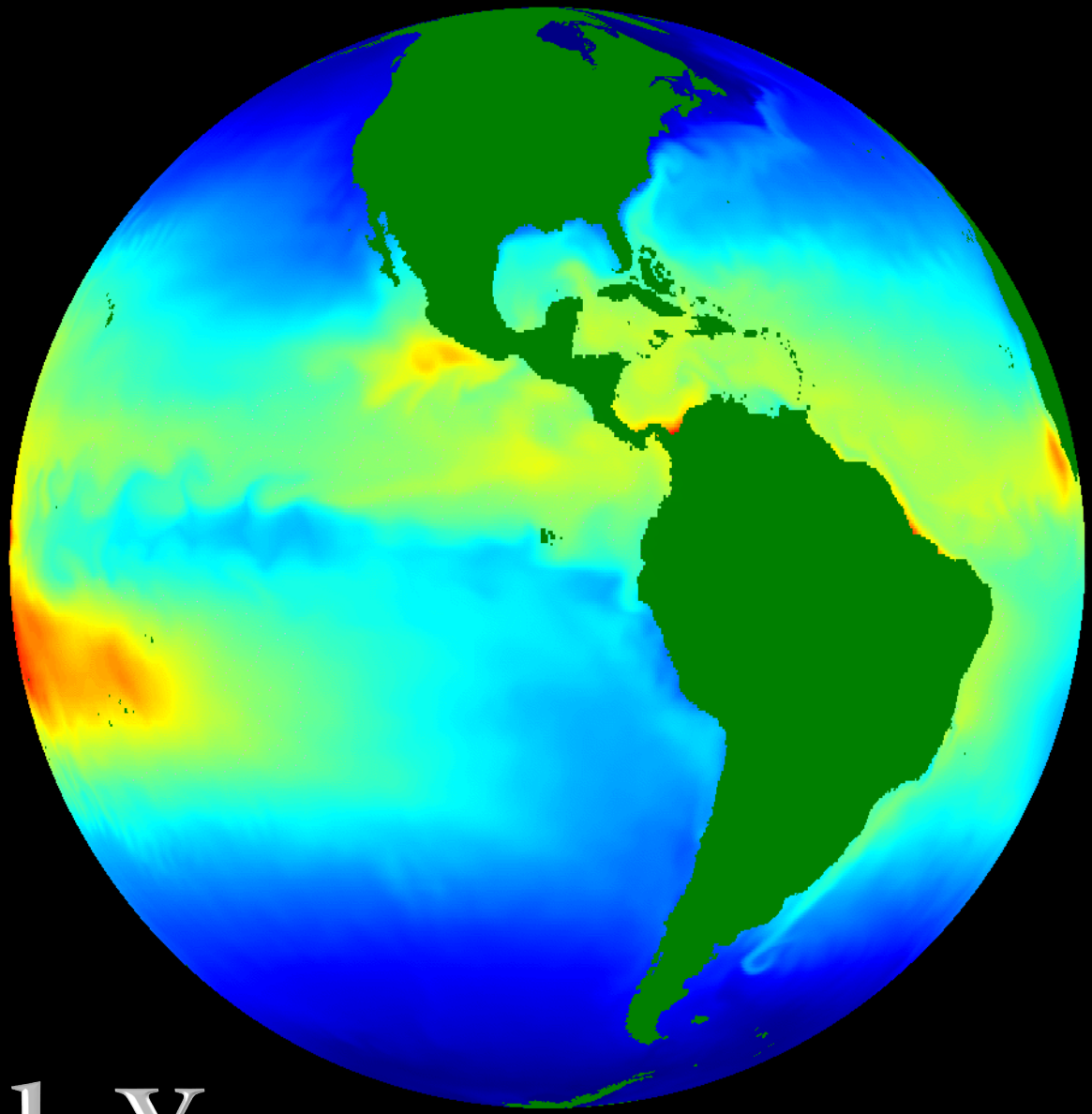

# Thank You